DEVELOPMENT OF COPOLYMER BASED SURFACE COATING WITH ANTIMICROBIAL ACTIVITY FOR GUTTA PERCHA AND INVESTIGATION OF ITS EFFICACY

A THESIS SUBMITTED TO
THE GRADUATE SCHOOL OF NATURAL AND APPLIED SCIENCES
OF ANKARA UNIVERSITY

by

Sena HAMARAT

IN PARTIAL FULFILMENT OF THE REQUIREMENTS
FOR THE DEGREE OF
MASTER OF SCIENCE IN
DEPARTMENT OF BIOMEDICAL ENGINEERING

ANKARA
2024

ABSTRACT

MSc Thesis

DEVELOPMENT OF COPOLYMER BASED SURFACE COATING WITH ANTIMICROBIAL ACTIVITY FOR GUTTA PERCHA AND INVESTIGATION OF ITS EFFICACY

Sena HAMARAT

Ankara University
Graduate School of Natural and Applied Sciences
Department of Biomedical Engineering

Supervisor : Prof. Dr. Hilal GÖKTAŞ

Dental health is one of the most important factors affecting the quality of life and daily activities of individuals today. Regular teeth cleaning and timely interventions by dentists help maintain a healthy structure, allowing individuals to continue their lives with their natural teeth. However, inadequate hygiene, unhealthy diets, and lack of regular check-ups can lead to dental decay, ultimately resulting in tooth loss. In this context, root canal treatment is applied to prevent tooth loss. Root canal treatment involves the removal of infected nerves, blood, and dead tissues from the root of the tooth, followed by filling the remaining space with a thermoplastic material called 'Gutta-Percha.' However, issues such as the degradation of the sealants used to bond Gutta-Percha to dentin, inadequate cleaning of the canals, and the growth of antibiotic-resistant bacteria may require the treatment to be repeated. The aim of this study is to prevent secondary treatments caused by these problems and to shorten the overall treatment duration. In this context, the surfaces of Gutta-Percha were coated with chlorhexidine and triclosan—materials proven to have antimicrobial properties in dentistry—using the 'Chemical Vapor Deposition' method, and their effectiveness against *E.coli* and *S.epidermidis* bacteria *in vitro* was examined. The *in vitro* studies showed that the coatings provided antimicrobial activity within the canal and acted as a primary protective barrier by repelling bacteria from the surface.

September 2024, 71 pages

Keywords : Gutta Percha, Antimicrobial Surface; Copolymer Coating; Chemical Vapor Deposition; Surface Coating; Root Canal Treatment.

ÖZET

Yüksek Lisans Tezi

GUTTA PERKA İÇIN ANTİMIKROBİYAL AKTİVİTEYE SAHİP KOPOLİMER ESASLI YÜZEY KAPLAMANIN GELİŞTİRİLMESİ VE ETKİNLİĞİNİN İNCELENMESI

Sena HAMARAT

Ankara Üniversitesi
Fen Bilimleri Enstitüsü
Biyomedikal Mühendisliği Anabilim Dalı

Danışman : Prof. Dr. Hilal GÖKTAŞ

Diş sağlığı günümüzde bireylerin hayat kalitesini ve günlük aktivitelerini etkileyen en önemli faktörleirn başında yer almaktadır. Dişlerin düzenli olarak temizlenmesi, gerektiği durumlarda diş hekimleri tarafından müdahale edilmesi ile sağlıklı yapının koruması kişilerin sahip olduğu dişlerle hayatlarını idame ettirmesine katkı sağlamaktadır. Ancak belirtilen hijyenin yeterli seviyede sağlanamaması, sağlıksız beslenme ve eksik kontroller neticesinde diş çürümesi ile başlayan problemler diş kaybına yol açmaktadır. Bu kapsamda kişilerin diş kaybını önlemek adına 'Kanal Tedavisi' uygulanmaktadır. Kanal tedavisi dişte bulunan enfekte olmuş ve çürük gelişimi gösteren sinir, kan ve ölü dokuların kökten temizlenmesi ve geride kalan açıklığın termoplastik bir malzeme olan 'Güta Perka' ile doldurulmasını kapsamaktadır. Ancak tedavi sürecinde, güte perkanın dentine tutunmasını sağlamak için kullanılan patların bozunması, kanalların yeterli seviyede temizlenememesi ve antibiyotiğe dirençli bakterilerin çoğalması gibi nedenlerden ötürü tedavinin tekrarlanmasını gerektiren durumlar meydana gelmektedir. Bu çalışmada amaç, bahsi geçen problemlerin sebep olduğu ikincil tedavinin önüne geçerek uzun süre tedavi süresini kısaltmaktır. Bu kapsamda güta perka yüzeyleri, diş hekimliğinde antimikrobiyal özelliği kanıtlanmış klorheksidin ve triklosan malzemeleri ile 'Kimyasal Buhar Biriktirme' yöntemi kullanılarak kaplanmış ve *in vitro* ortamda *E.coli* ve *S.epidermidis* bakterilerine karşı olan etkinliği incelenmiştir. Yapılan *in vitro* çalışmalarda kaplamaların kanal içerisinde antimikrobiyal etkinlik sağladığı ve kaplamaların bakterileri yüzeyden iterek birincil koruma kalkanı sağladığı görülmüştür.

Eylül 2024, 71 sayfa

Anahtar kelimeler : Guta perka; Antimikrobiyal Yüzey; Kopolimer Kaplama; Kimyasal Buhar Biriktirme; Yüzey Kaplaması, Kanal Tedavisi.

FOREWORD AND ACKNOWLEDGEMENT

As a beginning I would like to thank to my supervisor dear Prof. Dr. Hilal GÖKTAŞ, throughout my studies and research he was always guiding, helping, and encouraging me no matter what the results were. With the help of his support, I've managed to understand a substantial method in coating techniques, chemical analysis methods and how to properly write a project proposal. It was such a great and once in a lifetime experience to be a part of an amazing laboratory team, hoping to achieve many more successes together.

Sincere thanks and gratitude to dear Prof. Dr. Jülide Sedef GÖÇMEN, for her never-ending support and help during the microbiology experiment. I'm grateful to Dr. Kübra ERKAN TÜRKMEN, Prof. Dr. Hikmet KATIRCIOĞLU, Prof. Dr. Meltem DARTAR ÖZTAN and Dr. Emine ODABAŞI TEZER for their guidance about explanation and understating of thesis composition of the thesis, microbiology results and cytotoxicity analysis. Special thanks to dear Dr. Hatice Ferda ÖZGÜZAR, she made a great change in my perspective on life and academia, helped me both mentally and emotionally and always been there for any kind of help. I'm looking forward to being like her as such a successful and inspiring woman in science.

I want to make exclusive thanks to my dear colleague and one of the biggest luck in life Res. Asst. Mustafa TÜFEKÇİ. He's one of the best people I've ever met in my life and I'm so grateful for this opportunity, he has always been an amazing supporter and lifesaver in any hardship I've had and always feels like I have special brother. Therefore, a very sincere thanks for everything. And lastly, absolute gratitude to my parent Nurhan HAMARAT and Ali Rıza HAMARAT for their unquestioned support in everything in my life. I've always felt their support in everything I decided to be in, whether it was successful or not they were the biggest and the most precious supporters in everything. Therefore, it's an honor to be your daughter and I'll always try my best to achieve my dreams.

Sena HAMARAT
Ankara, September 2024

TABLE OF CONTENTS

SYMBOLS AND ABBREAVITIONS

°C	Degree Celsius
cm	Centimeter,
g	Gram
h	Hour
mL	Milliliter
nm	Nanometer
µL	Microliter
CA	Contact Angle
CFU	Colony Forming Unit
CHX	Chlorhexidine
CVD	Chemical Vapor Deposition
FTIR	Fourier Transform Infrared Spectroscopy
McF	Mac Farland
PBS	Phosphate Buffered Saline
RCT	Root Canal Treatment
rpm	Revolutions per Minute
SEM	Scanning Electron Microscopy
TCS	Triclosan
ToF-SIMS	Time-of-Flight Secondary Ion Mass Spectrometry
TSA	Tryptic Soy Agar
TSB	Trypticase Soy Broth
UV-Vis	Ultraviolet Visible Spectrophotometry
WHO	World Health Organization
XPS	X-Ray Photon Spectroscopy

LIST OF FIGURES

LIST OF TABLES

1. INTRODUCTION

Oral care and health play a crucial role in the quality of daily life, every person needs to feel comfortable and confident while talking, smiling, and eating because the mouth is one of the main body parts contact with the outside world. In order to maintain quality of life, proper oral care should be one of the priorities for each person. Mouth embodies several structures at ones for instance teeth, tongue, palate, cheek, gum, epiglottis etc. and each of them serves different function. Any kind of damage to one or the other has a direct effect on the remaining ones therefore, decent wellness underlies the proper function of each element. Especially, the fact that as living creatures we get our energy from food which firstly contacts with mouth, if a person cannot chew or swallow properly it can lead to even depravation in energy levels any other health problems.

In today's society, there are many factors affecting human health including air quality, cleanness of food, yet the ones with major affect are the food and water we consume. During consumptions both of the sources contact firstly with mouth then they follow the path to the other organs. In course of chewing, teeth come into play since they are the first processor for swallowing and digestion. However, teeth with less stability and strength may not serve a decent function. One of the main causes of such problems comes from dental caries. From research there were nearly 3.1 billion cases detected from 1990 to 2019, the main issue with these rates is that caries develop on permanent teeth (Qin et al., 2022). If left untreated caries tends to cause pain, swelling on gum and formation of infection since there are 700 microorganisms have been detected in oral flora (Haque et al., 2019; Selwitz et al., 2007). As different types of bacteria start to accumulate on tooth surfaces and colonize they build 'biofilms', and with the nutrients found in saliva they preserve their life cycle (Deo & Deshmukh, 2019; Faran Ali & Tanwir, 2012). Biofilm formation leads to plaque building up on tooth surfaces which causes gingivitis and periodontitis and if necessary precaution disregarded it can lead to teeth loss.

Among different microorganisms' certain bacteria step forward due to their role in tooth caries and loss and they are *Streptococcus mutans, Streptococcus sobrinus, Actinomyces odontolyticus, Streptococcus mitis, Fusobacterium necrophorum, Escherichia coli,*

Klebsiella pneumoniae, Candida albicans, Staphylococcus epidermidis, etc. (Yadav & Prakash, 2017). Mainly bacteria differ in their gram strains, for instance, *Streptococcus mutans* is a gram positive bacteria and *Fusobacterium necrophorum* is a gram-negative bacterium however they all take a role in tooth decay.

Over time, the prevalence of bacteria cannot be reversed, and the infection spreads out to tooth canals and roots and patients face to loss of their teeth. In dentistry healthcare professionals, pay attention to protect and save patients original teeth. This is because when a tooth is removed from the jaw the remaining teeth can lose their integrity/unity therefore the alignment can be lost, when a tooth is removed the soft tissue connecting it to the jaw becomes exposed to microorganisms the development of infection becomes inevitable and one of the other reasons is to protect patients from further procedures (Ghahramani et al., 2022). This means, if a tooth tried to be substituted with an implant there is a possibility of patients' tissue to not accept it and cause further pain, swelling and additional operations. To avoid such issues, protection of natural teeth is and substantial issue. Throughout the years various methods have been promoted from restoring materials such as gutta percha, foils, cement, and amalgam (Chandler, 2010).

Root Canal Treatment (RCT) is one of the most common methods for tooth preserving. In simple words, RCT is the removal of damaged or cannot be rescued from the roots, disinfection of the remaining tissue and filling the vacant space with thermoplastic material known as gutta percha (Banci et al., 2023). However, during the disinfection procedure complicated structure of teeth and the spreading of microorganisms to nearly every corner make it gruelling to remove fully (Sasser, 2020).

In this study, a new perspective for treatment has been proposed. The basics of the study are based on developing an antimicrobial protective layer around gutta percha surface which is the material that fills the vacancy left by cleaning. One of the main reasons for such purpose is to protect both soft and hard tissue of tooth from being invaded by microorganisms. Since, as mentioned earlier the prevalence of microorganisms causes tooth decay and if they're not being removed totally or if their spreading cannot be prevented they will spread to other tissues, they proliferate and cause biofilm formation.

For this reason in this study, triclosan (TCS) and chlorhexidine (CHX) have been synthesized as thin films on the gutta percha surfaces. Oxidative Chemical Vapor Deposition method had been preferred for film synthesis and antimicrobial activity of coatings had been tested with *S.epidermidis* and *E.coli*.

As a result of microbiological analysis, the co-polymeric structure of CHX – TCS coatings proved to be effective against bacterial spreading. The results were supported by the zone of inhibition test, in each test bacteria were expelled from gutta percha surfaces with an additional zone.

According to successful results, with additional improvements, coating can be applied to gutta percha surfaces and has a great potential to be commercialization.

2. LITERATURE SURVEY

2.1 Prevalence of Tooth Decay

General health is one of the key influences in everyday life, with proper health a person can fullfil his/her daily tasks and can have decent quality of life. Among many effectual elements, oral health has an extensive effect from smiling, eating, having conversations with other individuals, etc. Additionally, its significance has attracted the attention of World Health Organization in a worldwide research in 2003, and the welfare of the individuals have been emphasized as oral health is directly related to social relations and interaction of other systems in the human body (Petersen et al., 2003). Activities affected by oral health include insufficient digestion of food, cardiovascular and kidney health, and even diabetes (Dorfer et al., 2017).

As might be guessed, tooth decay is the most threatening and prevalent health concern against oral health. Depending on the wealth level of countries the ratios might differ yet, today 50% of the whole world's society is estimated to be affected by tooth decay. This data raises a concern and stands out as something to be careful about.

2.2 Formation of Tooth Decay

Teeth are composed of three main structures; enamel, dentin and pulp (Morris & Tadi, 2024). Enamel covers the outer part which is visible from the outside, is non-living tissue, first part contact with food and drinks yet, it is the hardest part of the whole structure. Dentin is the first living tissue underneath the enamel, and covers tissues from the end of the enamel till the roots, also hard tissue but not as hard as the enamel and contains small tubules responsible for sensitivity to outside stimulants if the enamel part gets damaged microleakages will be felt by the person. Inside the dentin, there is pulp, which is one of the crucial parts in charge of innervation and nourishment of the dentin also includes the constitution of dentin tissue by the function of odontoblast cells. It encapsulates nerves and blood vessels therefore it can provide food to teeth. The majority of pulp is water and only 20% is made from inorganic materials. The final part is the root canal, which is the

binding site between the gum and crown where all the nerves and blood vessels extend. These tissues have the potential to be house to microorganisms since the mouth has a moist environment, as person breathes oxygen and carbon dioxide are constantly circulated and food enters the body firstly from this orifice (Arola et al., 2017). Until now researchers have shown there are 700 various bacteria inhabiting the mouth (Deo & Deshmukh, 2019). Decays form when inhabitant bacteria inside the mouth, constantly have access to the nutrition and after consumption they produce enzymes and acids that are damaging to teeth (Kamay, 2015). Over time, the accumulation of enzymes and acids damages the inorganic components of the tooth and causes mineral loss which is the main constituent of the tooth. This impairment cannot be reversed yet, proper caring and routine control can bring under control.

2.3 Types of Bacteria Present in Tooth

As mentioned earlier, there were more than 700 various species of microorganisms have been detected in the mouth and oral cavities. Depending on the person's health level, there are plenty of bacteria that have a role in decay formation and root canal treatment. Research from several articles showed that the following microorganisms have a role in both decays and RCT's and they are; *Streptococcus mutans* (30% to 40%), *Lactobacillus species* (1% to 10%), *Actinomyces species*, *Streptococcus sobrinus, Enterococcus faecalis* (24% to 77%), *Fusobacterium nucleatum* (30% to 80%), *Prevotella intermedia* and *Prevotella nigrescens* (15% to 45%), *Porphyromonas endodontalis* (10% to 30%), *Candida albicans* (5% to 20%) (Gross et al., 2012; Marsh, 2010; Siqueira Jr & Rôças, 2009). Yet, following root canal treatment there are many cases of secondary root canal treatment. This is because even if canals have been sterilized with irrigants and other specific substances if bacteria weren't eradicated completely, it can repopulate and cause further damage in root and on GP. In this study, *Escherichia coli* (*E.coli*) from gram-negative family and *Staphylococcus epidermidis* (*S.epidermidis*) from gram-positive family have been studied in *in vitro* studies. *E.coli* was chosen due to its ubiquity in the human body, especially its habitat is the gastro-intestinal tract, the inner lining of the gut and intestines and has a great resistance to several antibiotics (Kibret & Abera, 2011; Rodrigo, 2020). By virtue of its persistence having a 3.7% prevalence in abscess

formation and 1.6% prevalence it also has a role in requiring secondary root canal treatment (Gajan et al., 2009; Siqueira et al., 2001). Besides, its incidence in the human body is one of the major influences of urinary tract infections drawing attention to its eradication. At the beginning of this study, it was mentioned that if *E.coli* can be eradicated with copolymer coating this may be applied to other surfaces where *E.coli* inhabits. Therefore, with this study, it was aimed to eradicate *E.coli* from gutta percha surfaces. One of the driving forces behind choosing *E.coli* was the applicability of the copolymer coating on different surfaces. As mentioned earlier, *E.coli* unfortunately causes the biggest percentage of infections in the urinary tract so if it can be eradicated from teeth roots and its coating on urinary catheters can provide further protection against infections.

Similarly, *S.epidermidis* was chosen mainly because of its role in the formation of secondary infection and due to its being gram-positive bacteria (Ooi et al., 2019). In literature, it's accepted as one of the bacteria living on human skin and in moist mucous surfaces and it's known for its existence in dental caries and spreading to pulps (Brescó et al., 2017; Devang Divakar et al., 2017). Particularly in cases of unsuccessful dental implant cases, the emergence of *S.epidermidis* with 17% prevalence is inevitable (Friedlander, 2010). The main reason for its unsuccessful eradication from surfaces comes from its resistance to antibiotics and since operation sites are highly susceptible to bacterial invasion it can hold on moist surfaces readily, proliferate and cause biofilm formation (Ooi et al., 2019). Due to the aforementioned reasons, *S.epidermidis* was chosen as the Gram-positive bacteria for study.

2.4 Decay Treatment

If decays can be determined before it's too late, the spreading of bacteria can be prohibited and therefore extension to other teeth can be restrained. Otherwise, it might even lead to the removal of the tooth including its roots and implant placement. As the implant is not a natural material there is a chance that patients' immune systems may not recognize it as biocompatible and can lead to inflammation and even removal. One of the renowned methods is 'Root Canal Treatment (RCT)' in which all the tissues contacted with

microorganisms including enamel and dentin (hard tissues), blood vessels and nerve tissues are taken out. Cleaning and filling the remaining vacancy with thermoplastic material called ‘gutta percha’ to protect the roots from unwanted sensitivity and also protect the tooth from further bacterial colonization.

If going over the procedure details, at the beginning the crown part has to be perforated to get into the pulp tissue. The depth of the opening starts from the enamel part until it reaches to end of the roots or where roots meet with gum. The reason for a deep opening is to be able to reach the nerves inside the tooth completely. When roots become visible, the cleaning part starts when all the pulp tissue including nerves and blood vessels is removed with tiny types of equipment and then the roots are shaped for proper filling and sealing (Estrela et al., 2014).

Then empty roots are filled with antibacterial fluids to kill or remove all the bacteria present inside the canals and therefore removed. If all the bacteria are not removed, the remaining ones can reproduce and cause a similar biofilm formation. When antibacterial fluid dries out, either one or multiple gutta perchas are filled in the roots with sealer around them. Shaping and handling of Gutta Percha is pretty easy due to its structure, when heat around 60^{o}C applied it starts to soften, further heating to 90^{o}C to 100^{o}C leads to melting and this helps to close all the openings inside the canals (Vishwanath & Rao, 2019). Additionally, sealer is meant to be an assistive element for gutta perchas since it enhances the binding between gutta perchas and dentin (Kaur et al., 2015). Depending on the number of roots of the tooth there can be multiple Gutta Perchas used for closure yet, sometimes only one Gutta Percha can be enough.

Following the treatment there are cases in the literature that end up with fails, the RCT fail ratios change between 7% to 18% (Jang et al., 2024). There are several reasons related to failures and the foremost substantial one is persistent bacterial colonies that were not fully eradicated (Bergenholtz, 2016). The complicated inner structure of the tooth and the limited ability of cleaning supplies might not be always enough for full cleaning therefore, even if a tiny bit of bacteria colony remains alive in the tooth it can spread to every place it can hold on. Another main reason is sealer cracking and dissolution, as mentioned

before sealers help to fill any untouched gaps in the canals over time their contact with saliva can cause disintegration and loss of bonding/integrity between gutta percha and roots (Siqueira, 2001).

As a result of the aforementioned reasons in this study, the protection of gutta percha surface with a multi-purpose coating was the starting point. In this context, Chlorhexidine (CHX) and Triclosan (TCS) have been coated as thin films on gutta percha surface with Chemical Vapor Deposition (CVD) method.

2.5 Chemical Vapor Deposition (CVD)

Surface coating term comprises a variety of techniques, if divided into headings as the state of the coating material the first one will be based on solution, the second one is molten or semi-molten, and the third one is gaseous vapor (Pinto et al., 2018). Sol-gel method, dip coating, spray coating, electrochemical coating, electrochemical coating, and slot-die coating are ranked under solution-based coating (Zhang et al., 2023). Thermal spraying, plasma spraying, cold spraying, arc wire spraying, welding and laser-based methods have been lined up under molten/semi-molten coating (Fotovvati et al., 2019). Lastly, ion beam deposition, chemical vapor deposition and physical vapor deposition methods are grouped under gaseous state deposition methods (Refai et al., 2020). Each method is used for different reasons such as the chemical structure of the coating material, the geometrical shape of the surface to be coated, the cost of the coating, etc., depending on parameters each technique serves advantages and disadvantages. In chemical vapor deposition, coating material has to be vaporized under a pretty low pressure environment (around 1.0 - 100 mTorr) so that it can controllably send on the surfaces (Hashmi, 2014). In the CVD method, samples are kept under vacuum conditions to prevent contamination, and the reactor walls have been heated to inhibit pilling up of coating material on walls. Additionally, when coating material has been vaporized it’s sent on the surfaces with needle valves for the adjustment of deposition thickness.

The main advantage of CVD are depositing a wide variety of materials and chemicals on every surface, meaning that the geometrical structure of the sample doesn’t affect the

coating. Additionally, as coating material has been vaporized it will be deposited homogeneously and highly pure on all surfaces under low temperatures (Doll et al., 2010). Since under vacuum conditions chemicals evaporate at lower temperatures than atmospheric conditions, this is quite helpful for both preserving the chemical structure of the material and being easily coated on surfaces (Noc & Jerman, 2022). Furthermore, vaporizing chemicals provide repetitive usage of the materials and therefore only a small amount of material is enough for coating. Due to vacuum conditions, possible impurities within the material easily being eliminated (Creighton & Ho, 2001).

CVD has also different types such as where if the polymerization takes place in oxidant presence (which is the main stimulant for polymerization) it's called oCVD, or if any initiator is used then called iCVD, if a plasma source used for chemical stimulation then it's called as Plasma Enhanced CVD (PECVD), if the reactor pressure is in quite high levels than called as Ultra High Vacuum CVD (UHVCVD), or if it's low than called as Atmospheric Pressure CVD (APCVD) (Fraga & Pessoa, 2020; Kumar et al., 2018).

In this study, the oCVD method has been used as it allows dry or solventless deposition on surfaces with conjugated structure (Borrelli et al., 2012). Besides, when samples in this case gutta perchas have been oxidized it helps vaporized monomers to be easily polymerized and adsorb on substrates (Dianatdar & Bose, 2023). Also, coating thickness is easily controlled and with high uniformity. Due to the nature of the method, coatings have been made under low temperatures. As an oxidant $FeCl_3$ has been used, and after polymerization oxidants have been removed from the surfaces with methanol easily.

2.6 Chlorhexidine (CHX)

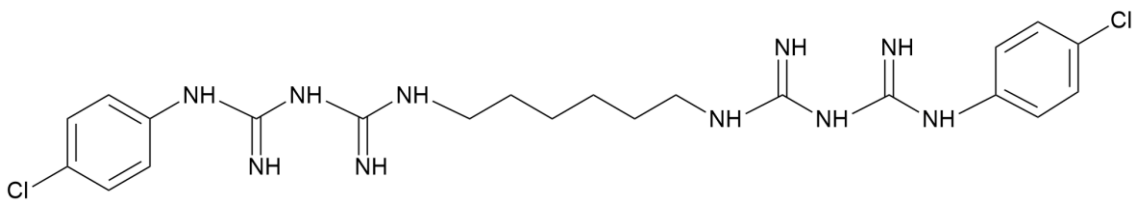

Figure 2.1 Chemical structure of chlorhexidine monomer

Chlorhexidine is a lab-grown chemical and it has been used as an effective disinfectant since then not only in dentistry but also in surgical tools (Poppolo Deus & Ouanounou, 2022). In the literature its virulent activity against gram-positive, gram-negative, fungi, yeast and viruses has been proven by many studies, this activity results from its ability to disrupt the membrane integrity of microorganisms (Roode & Butow, 2018). As chlorhexidine has a positively charged structure that attracts and binds to the negatively charged membrane of microorganisms, therefore after interaction intra-cellular content tends to be expelled to outside leading to cell death of microorganisms (Milani et al., 2021). Chlorhexidine two in a one action, depending on its concentration can serve both bacteriostatic action which repels bacterial adherence on surfaces and also it provides bactericidal activity which kills all the bacteria it contacts with (Karpiński & Szkaradkiewicz, 2015).

As structurally, chlorhexidine contains both hydrophilic and hydrophobic groups structure therefore it can adhere to a variety of surfaces (Méndez-Vilas, 2011). Due to its effectiveness in the eradication of bacteria, prevention of plaque formation and gingivitis, and biofilm prevention CHX has a wide array of applications such as mouthwashes, root canal irrigants, toothpaste, dental implants, and as a disinfectant agent in medical equipments (Brookes et al., 2020; Jenkins et al., 1993; Poppolo Deus & Ouanounou, 2022; Shukla et al., 2014).

2.7 Triclosan (TCS)

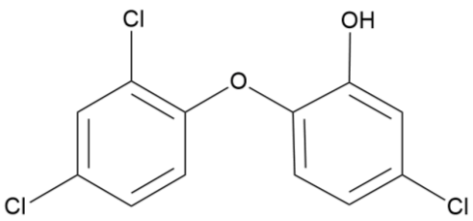

Figure 2.2 Chemical structure of triclosan monomer

Triclosan is another lab-grown chemical with a resemblance to CHX in both structural and antimicrobial activity, as seen from the figure above it is also composed of two benzene rings and contains chlorine. Just as CHX, it has the capability of eradicating bacteria by interfering with membrane lipid synthesis as a result of such action bacteria cannot complete their outer protective layer and the inner structural elements become exposed to the outside (Macri, 2017). The antimicrobial activity of TCS is not limited to bacteria only, it also includes fungi and protozoa (Sun & Textile, 2016). Due to its extensive antimicrobial activity, its usage areas are quite wide including toothpaste, mouth rinses, sterilizer as in the root canals, body washes, and in soap (Bhargava & Leonard, 1996). The study by Jongsma et al. in 2015 proved that TCS has the anti-biofilm capability on retainers when patients were required to use toothpaste and mouthwash with TCS additive results demonstrated the lowest colony formation (Jongsma et al., 2015).

2.8 Surface Analysis Techniques

2.8.1 Fourier transform infrared spectroscopy (FTIR)

FTIR is an analytical tool used for the identification of elemental composition and chemical bonds of any solid, liquid and gaseous materials (Dutta, 2017). In basic terms, a range of specific wavelengths of light is being sent to samples, inside the samples specific chemical bonds become excited by absorbing photons therefore this causes particular bonds to vibrate with specific frequency levels (Ismail et al., 1997). The difference between incident light and transmitted/absorbed light then being analyzed by the device and the resultant vibrational spectrum been displayed on the screen (Smith, 2011).

2.8.2 Ultraviolet visible near infrared spectroscopy (UV-Vis)

UV-Vis is similar to FTIR analysis, in this method the interaction between the light source and the sample are being measured in terms of transmittance, absorbance and reflectance as the light passes through the sample (Otsuki & ScienceDirect, 2024). With this

technique functional groups within the compound and the structural changes took place during interactions (Aslam et al., 2023). Additionally, due to the nature of the interaction of light with substances reestimation about the film thickness can be made (Dutta et al., 2022).

2.8.3 X-ray photon spectroscopy (XPS)

XPS is another identification tool used for labelling elements and potential chemical bonds from the sample surfaces. Different from FTIR, XPS provides quantitative information about the content of the sample. The quantitative information is related to the presence percentage of elements on the surface within 1 to 10 nm depth (Van der Heide, 2012). Regarding percentages, possible chemical bonds and composition of any material can be assigned. The technique operates as an X-Ray source that bombards the sample surface causing the emission of electrons depending on their binding energy levels which is characteristic of each element and its interaction with other elements (Stevie & Donley, 2020). Each electron breaks off from a specific orbital from the element and this causes a release of kinetic energy, the detection of this kinetic energy with the number of the same energies is detected and displayed by the device (Watts, 1994). Additionally, surfaces with multiple layers can also be analysed with this method since it provides depth profiling therefore the composition of a sample can be precisely revealed (Hofstetter & Vaynzof, 2019).

2.8.4 Scanning electron microscopy (SEM)

SEM unlike previous techniques is a three-dimensional topographical analysis technique that provides morphological properties with high resolution ranging from micron to nano scales (Inkson, 2016). Additionally, SEM analysis provides images with different magnifications ranging from 10x to 1000000x which is the main detailing tool (Mohammed & Abdullah, 2018). Topographical properties like shape, purity, homogeneity and particle sizes can be all ascertained from the scans (Karak, 2019). Therefore, it's a quite useful tool for surface property analysis. It's been used in material sciences, biology, metallurgy, nanotechnology, archaeology, geology, etc., therefore it's

quite a useful tool for morphological analysis (Worsfold et al., 2019). In the technique, samples are divided into two groups, the conductive ones and the non-conductive ones. The majority of the non-conductive surfaces have been coated with gold or carbon materials for the improvements of surface details. During the analysis samples were kept under a vacuum condition to prevent the interaction of electron with air (Minuti et al., 2022).

3. MATERIALS AND METHODS

3.1 Materials

Table 3.1 Materials used during sample preparation

SAMPLE PREPARATION		
Materials	**Brand**	**Purpose of Use**
Gutta percha	Sure Dent Corporation	Microbiological analysis.
Glass slide	ISOLAB	Experimental surface coating and XPS sample surfaces.
Silicon wafer	SIEGERT WAFER	Experimental surface coating, ToF-SIMS, and SEM sample surfaces.
70% Ethanol	ISOLAB	Sample surface cleaning.
Chlorhexidine (≥ 99.5%)	Sigma-Aldrich	Synthesizing of copolymer coating.
Triclosan (≥ 99.79%)	Aklar Kimya	Synthesizing of copolymer coating.
Iron (III) chloride/FeCl3	Sigma-Aldrich	Oxidant for thin film synthesis.
Spatula set	ISOLAB	Measuring, and transferring monomer during experimental preparation.
Forceps	ISOLAB	Gripping, placing and transferring samples from sample holder to petri dishes.
Filter Paper	ISOLAB	Drying samples and protecting from contaminants.
Gloves	Dolphin	Protection of hands from chemicals and preserving samples from contamination.

Table 3.2 Materials used during thin film coating

THIN FILM COATING		
Devices	**Brand**	**Purpose of Use**
Chemical Vapor Deposition (CVD)	Kenar Mühendislik	Synthesis of copolymer thin films on sample surfaces.
Vacuum pump	Vacuubrand VAP5	Evacuating air trapped inside the CVD reactor.
Cold trap	CLS CLCT -40	Trapping excessive chemical vapor from getting into pump.
Chemical storage tubes	Çalışkan Laboratory	Storage of monomer chemicals.
Vacuum Glass Desiccator	ISOLAB	Storage of samples for the prevention of contamination.
Vacuum Drying Oven	ILDAM	Storage of samples for the prevention of contamination.

Table 3.3 Materials used during microbiological experiments

MICROBIOLOGY EXPERIMENTS		
Materials / Devices	**Brand**	**Purpose of Use**
Staphylococcus epidermidis ATCC 35984 (Standard strain)	American Type Culture Collection	Analysing the effect of antimicrobial properties of copolymer thin films.
Escherichia coli ATCC 25922 (Standard strain)	American Type Culture Collection	Analysing the effect of antimicrobial propertiese of copolymer thin films.
McFarland Densitometer	BIOSAN – DEN-1	Concentration measurement of bacterial suspension

Table 3.3 Materials used during microbiological experiments (continued)

Test tubes (Borosilicate)	BIOSAN	Storage of bacterial suspension for concentration measurement
Tryptic Soy Broth	Merck 105459.0500 Tryptic Soy Broth For Microbiology	Liquid feedlot for bacteria and their storage environment.
Tryptic Soy Agar	Merck 105458.0500 Tryptic Soy Agar For Microbiology	Solid feedlot for bacteria and their inoculation surface.
Centrifuge Tubes (2 ml) – Gamma Sterile	ISOLAB	Storage of gutta percha samples incubated with bacteria suspensions.
Centrifuge Tubes (50 ml) – Gamma Sterile	ISOLAB	Preparation of bacterial suspension.
Vortex (0 ~ 3000rpm)	Fine Vortex (FINERPCR)	Diffusing bacteria suspension homogeneously.
Incubator	Memmert (IN110, +5°/+80°)	Storage of bacterial suspensions and inoculated samples.
Precision Balance	BEL	Weighting
Magnetic Stirrer	Heidolph	Homogenize both feedlots
Erlenmeyer Flask (1000 ml & 500 ml)	S & H Labware Boro 3.3	Preparation of Tryptic Soy Agar and Broth
Graduated Cylinder (1000 ml)	S & H Labware Boro 3.3	Preparation of Tryptic Soy Agar & Broth
Micropipettes (10 – 100 µl, 20 – 200 µl, 100 – 1000 µl)	ISOLAB	Measurement and transfer of liquids
Micropipette tips (10 – 100 µl, 20 – 200 µl, 100 – 1000 µl)	ISOLAB	Prevention of contamination and mixing of concentrations.
Washing Bottle (500 ml)	ISOLAB	Storage of ethanol, methanol, deionized water.

Table 3.4 Devices used during surface/sample analysis

ANALYSIS DEVICES		
Devices	**Brand**	**Purpose of Use**
FT/IR Spectrophotometer	JASCO (4700 Spectrophotometer)	Spectral chemical bond analysis of thin films (coatings made on silicon wafer).
UV-Vis Spectrophotometer	JASCO (V-750 Spectrophotometer)	Spectral chemical bond analysis of thin films (coatings made on glass slides.).
X-Ray Photoelectron Spectrometer (XPS)	PHI 5000 VersaProbe (METU - MERLAB)	Depth profile analysis of sample surfaces in order to detect presence of chemical bonds.
Time of Flight-Secondary Ion Mass Spectrometer (TOF-SIMS)	ION-TOF ToF-SIMS 5	Polymeric weight analysis and detection of copolymer structures.
Scanning Electron Microscope (SEM)	QUANTA 400F Field Emission SEM	Topographical analysis of samples with high resolution in nanometre scale.

3.2 Methods

3.2.1 Sample sterilization

In the preparation of experiments, glass slides and silicon wafers with 1 x 2 cm^2 area and gutta perchas were sterilized with 70% ethanol, 3 times for 5 minutes. Then ethanol and residues were removed by washing samples with distilled water 3 times for 5 minutes. After all the cleaning samples were let to dry in the fume hood for 24 hours.

3.2.2 Experimental section

Before each experiment, samples that are going to be coated have been placed on metal plates with heat-resistant tapes. Placed on the CVD reactor in an upside-down direction in which the samples were facing the outlets of monomer vapor. When all the preparations

were completed, experiments started with the evacuation of air trapped inside the CVD reactor. During evacuation reactor walls were heated to 50ºC to avert monomer accumulation on walls. When the pressure level dropped to 120 mTorr, oxidant and monomer/monomers were heated up gradually. At first oxidant $FeCl_3$ was heated from 60ºC to 250ºC gradually by 20ºC per increment so that the solid particles wouldn't blast everywhere. For TCS it was heated from 60ºC to 125ºC and for CHX it was heated from 60ºC to 165ºC. When both monomer and oxidant reached their ideal degree's stopwatch was set to 2 hours. When the 2-hour period was over, samples were taken out of the reactor and stored in the desiccator until the time when it'll be used for bacterial inoculation.

3.2.3 Bacteria feedlot preparation

As a feedlot, both liquid and solid forms were prepared. Tryptic Soy Agar (TSA) and Tryptic Soy Broth (TSB) were prepared as solid and liquid feedlots, respectively. For TSA medium, 40 g of it was weighted and mixed with distilled water up to 1L of solution prepared. For full dissipation, a magnetic stirrer was used for 5 minutes at 720 rpm. Similarly, for TSB medium, 15 g was mixed with 500 mL distilled water and magnetic stirrer was used for full blending.

Both of the mediums cannot be used as prepared since, without sterilization any kind of liquid can contain undetectable microorganisms. To avoid for such a probability all the mediums were sterilized in an autoclave at 120ºC for 20 minutes.

Following the sterilization TSA medium was poured into Petri dishes in 4 mL volumes and let to dry completely. After drying both TSA and TSB were placed into the fridge at 4ºC for long term usage.

3.2.4 Bacterial inoculation

In the first step, samples were separated into 2mL centrifuge tubes individually. The bacterial suspension was prepared with tryptic soy broth (TSB), centrifuge tubes and fresh bacterial passage. Firstly, 3 ml TSB was poured into the centrifuge tube then a swab was

used to smear a small amount of bacteria from passage agar then it was mixed with TBS. To mix, all the bacteria centrifuge tubes were placed on the vortex and mixed for 15 seconds. After this, the concentration of the suspension was analysed with a McFarland Densitometer. When centrifuge tubes having bacterial suspensions were placed inside the densitometer, it had to be between 0.5 to 0.6 Mc in other words, approximately it has 1.5 x 10^8 density of cells. For the sake of proper handling of samples and proper bacterial counting the concentration of suspension was diluted with 1:100 rate. The dilution was necessary to count cells properly and precisely. After preparing the bacterial suspension, it was distributed to all centrifuge tubes as 1 mL and then all the samples were put in an incubator with 37ºC and 10% moisture room conditions.

Figure 3.1 Microbiology studies were performed in Class II - B Type Biosafety Cabinet

3.2.5 Agar incubations

The incubation period was divided into 4 days; 1, 3, 7 and 15. In each according time samples were incubated in agar surfaces. Firstly, samples were taken out from incubator, then they were taken into microbiology safety cabinet. In the cabinet, the first was preparations of feedlots. Bacterial feedlots in this case TSB were the subject, it was poured into empty and sterilized 2 mL centrifuge tubes. The amount was changing from

900 µL to 1000 µL. Additionally, PBS solution was also poured into empty and sterilized 2 mL centrifuge tubes as a cleaning and preparation solution. Then samples were taken out from their initial centrifuge tubes and placed into fresh PBS solution. In this step, the main purpose was to remove bacteria that was not able to hold on to gutta percha surfaces, to do this gutta perchas were gently washed for 3 times and then they were transferred to fresh TSB medium. Following this step, both TSB and PBS suspensions were diluted for agar cultivation. The dilution ratios were changing from 10^{-1} to 10^{-13} this dilution was necessary for precise bacterial counting. The dilutions were prepared with TSB solution. After dilutions were completed, bacterial suspensions were cultivated on agar plates. Agar surfaces were separated into 4 sections because the last four dilutions were the most accurately countable ones.

Agar cultivation was done as 100 µL with micropipettes. In each section corresponding centrifuge tube was vortexed for seven seconds to make sure that suspension had a homogenous form. Following mixing new pipette tips were used for each dilution. When cultivations were done, agar plates were placed into incubators for 24 hours at 37°C with 10% humidity.

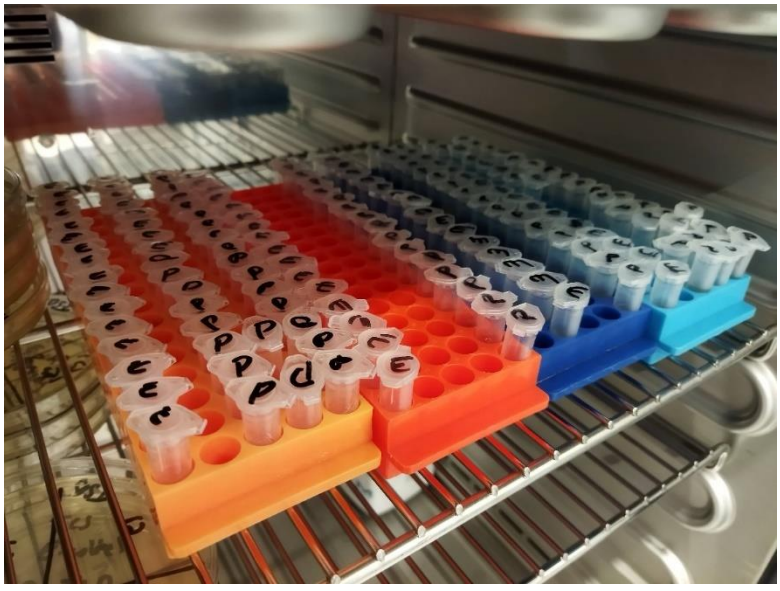

Figure 3.2 Samples were placed in the incubator for bacteria-sample interactions

3.2.6 Bacterial counting

Bacterial colonies were counted from agar plates after 24 hours to be able to count them as an un-equipped naked eye. Counting was done from the dilution where all the colonies were visualized and the number from that section was multiplied with its dilution constant.

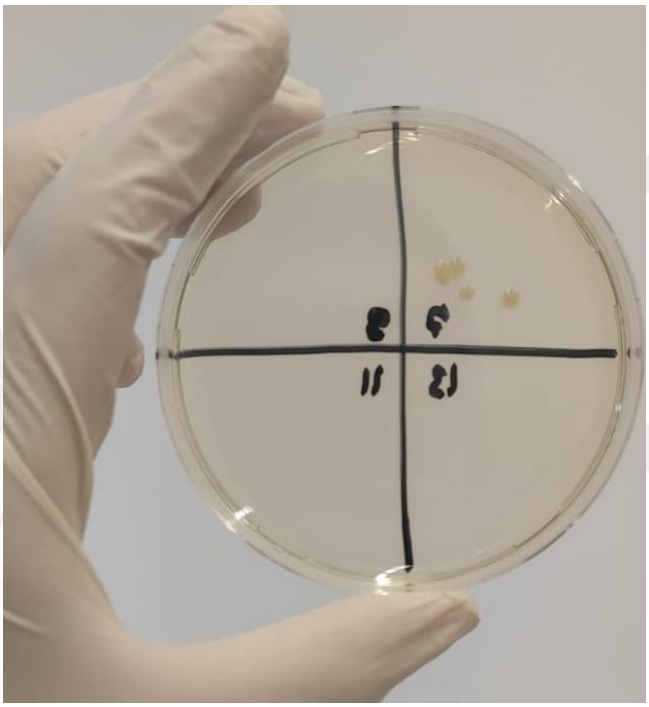

Figure 3.3 Colonies formed after 24 hours incubation

3.2.7 Zone of inhibition test

During bacterial inoculation on agar plates, agar inhibition zone analysis was also performed. For tests, bacterial suspension with $1.5x10^6$ CFU/mL concentration was prepared and 500µL was inoculated on every agar plate. With the help of inoculation loops, all the suspensions were spread out homogeneously, then coated gutta percha samples were left on agar surfaces at a distance. Following the first 24 hours of incubation agar surfaces were photographed until the 15^{th} day.

3.2.8 Cytotoxicity analysis

In vitro cytotoxicity studies were conducted using the L-929 mouse fibroblast cell line following ISO 10993-5 standards (ISO, 2022). The primary goal of these tests was to determine whether CHX-TCS thin film-coated glass slide samples had any potential harmful effects on living tissue. To accurately detect any changes in the metabolic activity of the cell line, MTT assay analyses were performed.

The cells used in the experiment were first revived in a medium prepared at standard concentrations and then cultured in flasks to prepare them for contact with the coated catheter samples. The cells, cultured for 24 hours under conditions of 37°C and 5% CO2, were detached from the flask surface using a solution of 0.25% trypsin and 0.05% EDTA, ensuring equal distribution into 24-well plates. To prevent cytotoxicity, DMEM was added to the medium, and after centrifugation, the trypsin-EDTA solution was removed. The cells were then resuspended in DMEM and distributed into the wells.

The seeded cells were incubated for 24 hours to allow them to adhere and proliferate. After 24 hours, any unattached or dead cells were removed during the DMEM media change. To compare the effects of the coated catheter samples on cell viability, uncoated catheters were used as the control, with commercial tissue culture polystyrene (TCPS which was named ‘Control’ in the results part) serving as the negative control.

After incubation, the thin film-coated glass slides were added to the wells containing the cultured cells and incubated for 24 hours. To analyze the effect of the coated glass slides on cell viability, 0.5 mg/mL MTT was added to the wells and incubated for 4 hours to allow interaction with the cells' metabolic activity. After incubation, the cells were washed, and the formazan crystals formed in the MTT-interacting cells were dissolved in 500 µL of DMSO. Finally, the absorbance values at the characteristic wavelength of 540 nm were measured using a Thermo Scientific Multiskan GO Microplate Photometer to calculate the ratio of dead to live cells. Cytotoxicity analysis have been repeated for 5 times for each sample in order to reach the highest accuracy.

4. RESULTS AND DISCUSSION

4.1 Surface Characterization

4.1.1 FTIR analysis

In the thin film synthesis, TCS and CHX thin film were firstly synthesized on glass slides and silicon wafers as control samples. To see is there any changes take place within the structure of monomer molecules when interacting with $FeCl_3$ molecules under CVD conditions. Following the polymerizations FTIR scan of samples was taken and residual $FeCl_3$ molecules were washed with methanol. This step was necessary for the elimination of inert $FeCl_3$ residues on the surfaces that were able to adsorb along with non-polymerized TCS monomer molecules.

In the first image, the TCS monomer has been demonstrated (Figure 4.1). The corresponding chemical bonds have been framed with colored rectangles and numbered. Respectively, colored rectangle corresponds to (1) -OH bond between 3472 cm^{-1} – 3250 cm^{-1}, (2) Benzene ring between 3230 cm^{-1} – 3010cm^{-1}, (3) -CH/-CH_2 stretching between 2972 cm^{-1} – 2844 cm^{-1}, (4) -C=C- stretching of the aromatic ring between 1638 cm^{-1} – 1371 cm^{-1}, (5) -C-C stretching between 1371 cm^{-1} to 1274 cm^{-1}, (6) -C-O-C- stretching between 1274 cm^{-1} – 1048 cm^{-1}, (7) -C-Cl stretching between 957 cm^{-1} – 831 cm^{-1} and finally (8) -C-H stretching or aromatic ring between 831 cm^{-1} – 532 cm^{-1} (Aminu et al., 2021; Celebioglu et al., 2014; Lou et al., 2014; Pavia et al., 2015; Querido et al., 2021; Stuart & ProQuest, 2004).

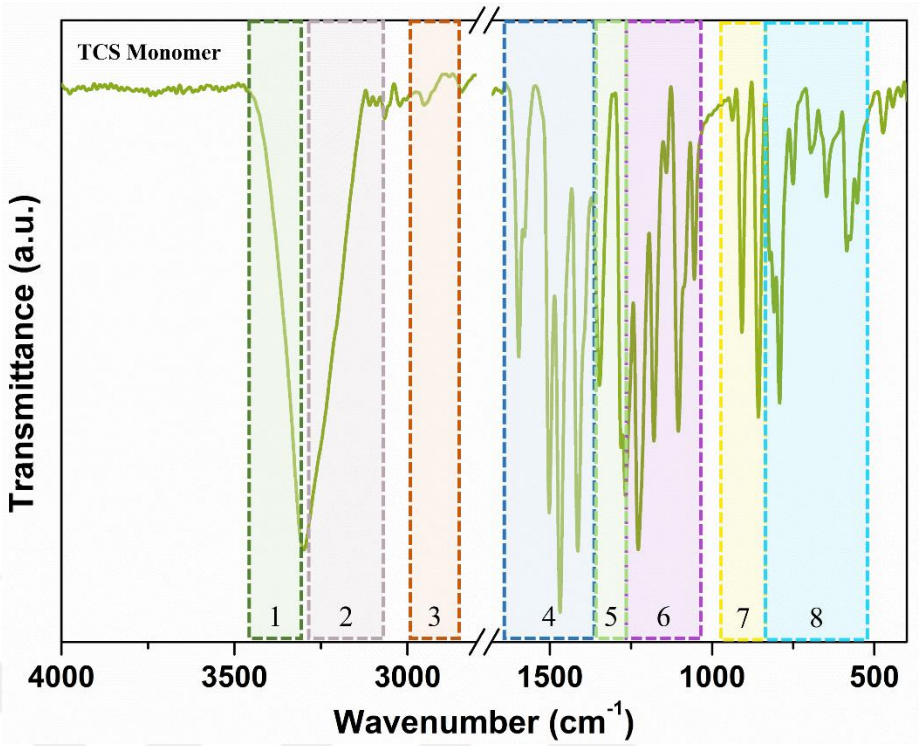

Figure 4.1 FTIR spectra of triclosan monomer

The following spectrum image seen in Figure 4.2 is the TCS film on silicon wafers. TCS thin films were synthesized by evaporating the TCS monomer at 125°C and reacting the monomer with $FeCl_3$ for two hours with the base pressure 100mTorr and 20mTorr pressure difference as a result of vaporized monomer. As seen from Figure 4.2, through polymerization process the main structure of TCS has been mostly preserved, only differences seen in transmittance reduction in the aromatic ring and the prominent reduction of C-Cl and C-H bonds again they've not utterly been broken during polymerization yet, majority of them have been used for new bond formation.

The corresponding bonds detected on the films are (1) -OH bond between 3680 cm^{-1} – 3250cm^{-1}, (2) Benzene ring between 3216 cm^{-1} to 3010 cm^{-1}, (3) -CH/CH_2 stretching bond between 2980 cm^{-1} – 2759 cm^{-1}, (4) -C=C- aromatic ring between 1675 cm^{-1} – 1371 cm^{-1}, (5) -C-C- stretching between 1371 cm^{-1} – 1183 cm^{-1}, (6) C-O-C bound between 1176 cm^{-1} to 1022 cm^{-1}, (7) C-Cl stretching between 960 cm^{-1} to 825 cm^{-1}, and finally (8) -CH stretching of aromatic bond between 760 cm^{-1} to 569 cm^{-1} (Aminu et al., 2021;

Celebioglu et al., 2014; Lou et al., 2014; Pavia et al., 2015; Querido et al., 2021; Stuart & ProQuest, 2004).

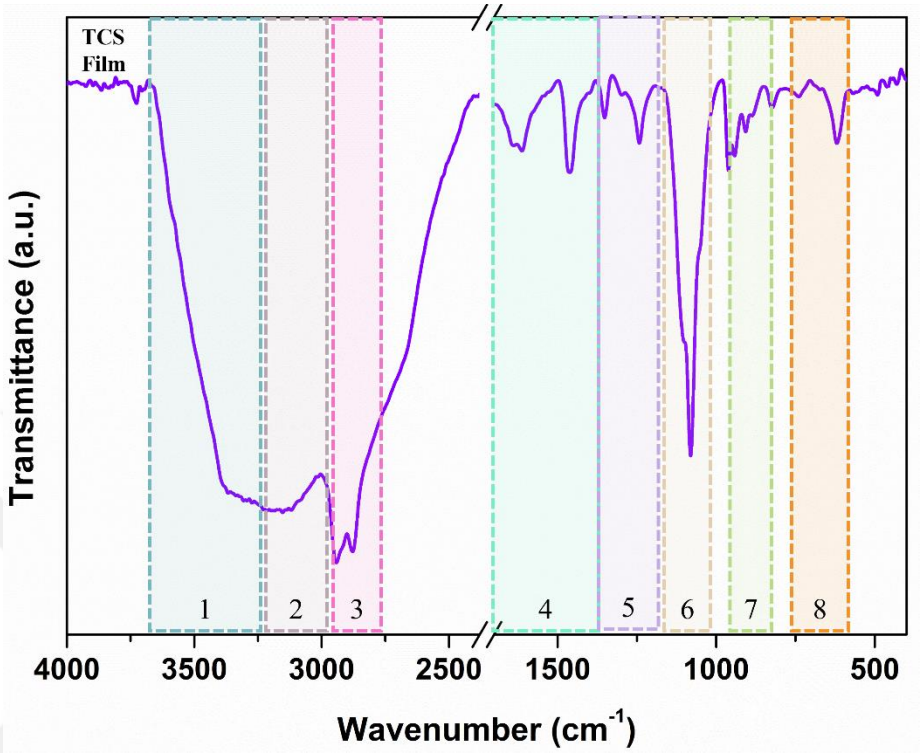

Figure 4.2 FTIR spectrum of triclosan thin film

The following Figure 4.3 is an FTIR image of TCS thin film from a silicon wafer which was washed from $FeCl_3$ residues with methanol. When both the original TCS thin film and the methanol-washed samples were compared, it's evident that the main structure of the thin films was quite similar yet, the width of the C=C bond seems to be confined with a reduced aromatic ring band. Even though few changes have been detected in the thin films, the main polymeric structure of the thin films remains. Since (1) -OH bond has been seen between 3583 cm^{-1} – 3134 cm^{-1}, (2) Benzene ring between 3120 cm^{-1} – 3010 cm^{-1}, (3) -CH/-CH_2 bond between 2966 cm^{-1} – 2811 cm^{-1}, (4) -C=C- aromatic ring between 1514 cm^{-1} to 1306 cm^{-1}, (5) -C-C- stretching between 1280 cm^{-1} to 1188 cm^{-1}, (6) -C-O-C bond between 1165 cm^{-1} to 989 cm^{-1}. (7) C-Cl stretching between 969 cm^{-1} to 822 cm^{-1} and finally (8) C-H stretching of 778 cm^{-1} to 578 cm^{-1}.

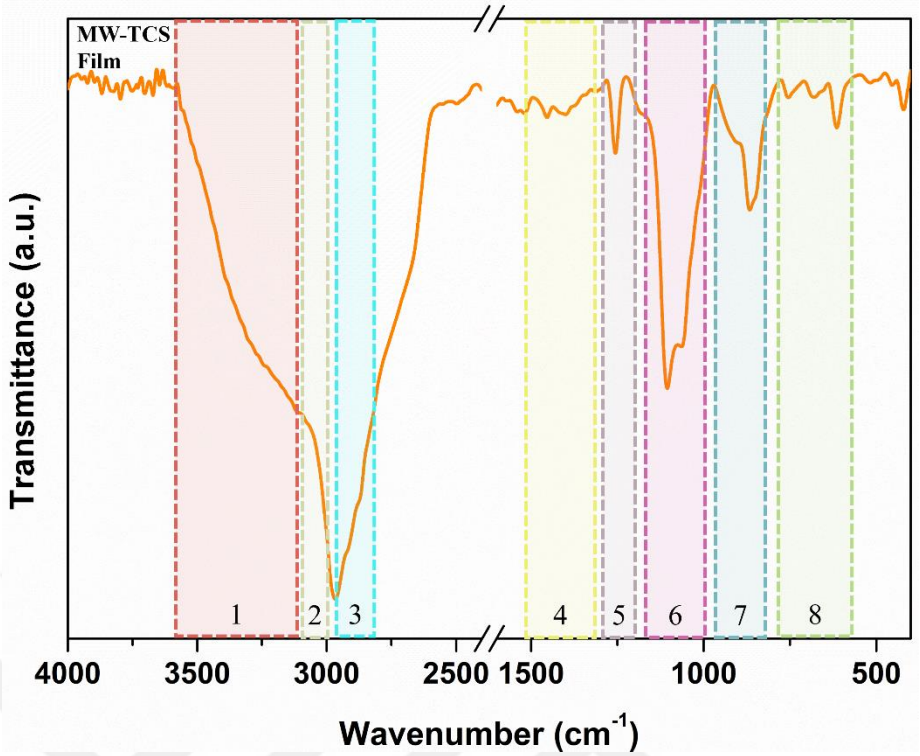

Figure 4.3 FTIR spectrum of triclosan thin film after rinsed with methanol

The following Figure 4.4 FTIR scan is CHX monomer. Characteristic chemical bond and peaks of CHX monomer was seen as (1) Primary -NH stretching vibration between 3539 cm^{-1} – 3284 cm^{-1}, (2) Benzene ring between 3251 cm^{-1} – 3011 cm^{-1}, (3) -CH/-CH_2 stretching vibration between 2986 cm^{-1} – 2746 cm^{-1}, (4) -C=N stretching vibration between 1702 cm^{-1} – 1641 cm^{-1}, (5) -C=C aromatic ring vibration between 1623 cm^{-1} – 1377 cm^{-1}, (6) -C-N and C-C overlapped stretching vibration between 1377 cm^{-1} – 1131 cm^{-1}, (7) C-Cl bond between 948 cm^{-1} – 783 cm^{-1} , (8) -CH stretching of aromatic ring between 752 cm^{-1} - 572 cm^{-1} (Bettencourt et al., 2023; Onnainty et al., 2016; Pavia et al., 2015; Priyadarshini et al., 2017; Stuart & ProQuest, 2004; Yang et al., 2007).

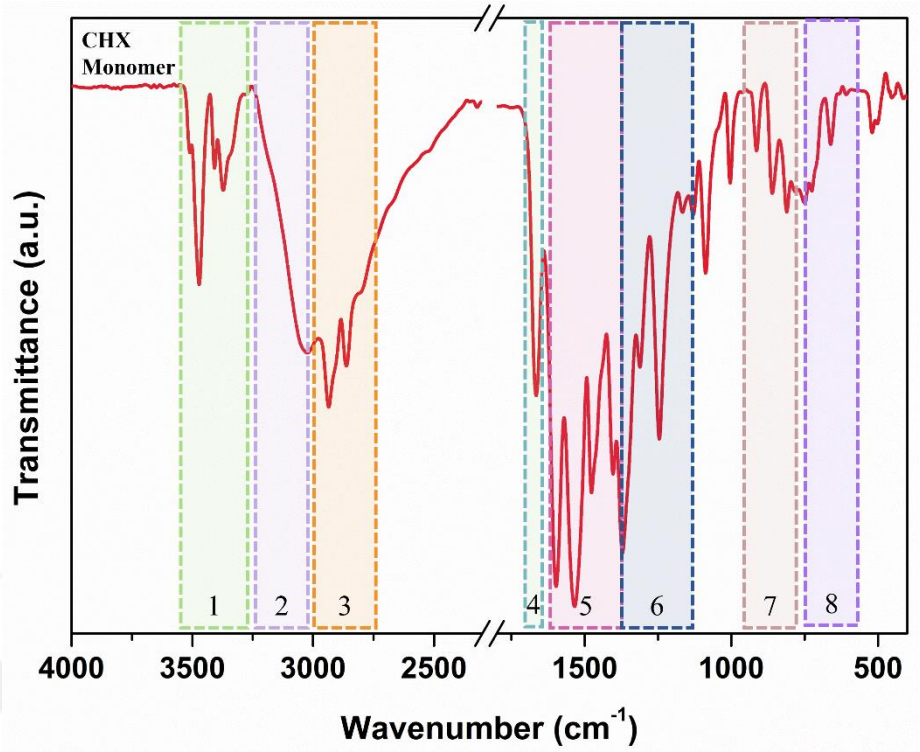

Figure 4.4 FTIR spectra of chlorhexidine monomer

The following FTIR spectrum (Figure 4.5) is the graph of CHX thin film synthesized on the silicon wafer. CHX monomers have been polymerized as thin films with oCVD method, under 100 mTorr base pressure and vaporized at 165°C and let to interact with $FeCl_3$ for two hours. When thin film peaks were analysed the majority of the peaks that were seen on the monomer were also marked on the thin film. However, as expected due to polymerization certain changes have also occurred on the thin film. The structure of the film lost the majority of the -NH bonding with the -C=N part yet, the remaining parts seem to be preserved during polymerization. Firstly, if bonds were pointed out respectively, (1) -OH bond between 3741 cm^{-1} – 3580 cm^{-1}, (2) Primary -N-H stretching between 3413 cm^{-1} – 3131 cm^{-1}, (3) Benzene ring 3099 cm^{-1} – 2988 cm^{-1}, (4) -CH/-CH_2 stretching between 2975 cm^{-1} – 2800 cm^{-1}, (5) -C=C- aromatic ring between 1477 cm^{-1} – 1326 cm^{-1}, (6) -C-N and C-C overlapped stretching vibration between 1312 cm^{-1} – 1027 cm^{-1}, and finally (7) -C-Cl stretching between 971 cm^{-1} – 731 cm^{-1}, (8) -CH stretching of aromatic ring between 670 cm^{-1} – 558 cm^{-1} (Bettencourt et al., 2023; Onnainty et al., 2016; Pavia et al., 2015; Priyadarshini et al., 2017; Stuart & ProQuest, 2004; Yang et al.,

2007). From the differences in peaks, it's quite clear that during polymerization majority of aromatic ring and -C-Cl were preserved yet, some of the monomers had reacted with the oxidant led to the breaking of -NH bond, aromatic ring and -C-Cl bond. Distinguishingly, other than the aforementioned bonds -C=N bond has been broken off almost completely. These missing chemical bonds lead to the idea that as -C=N bond breaks those vacancies were completed with C-H bonds to stabilize the excited state and make a covalent bond on the sample surfaces.

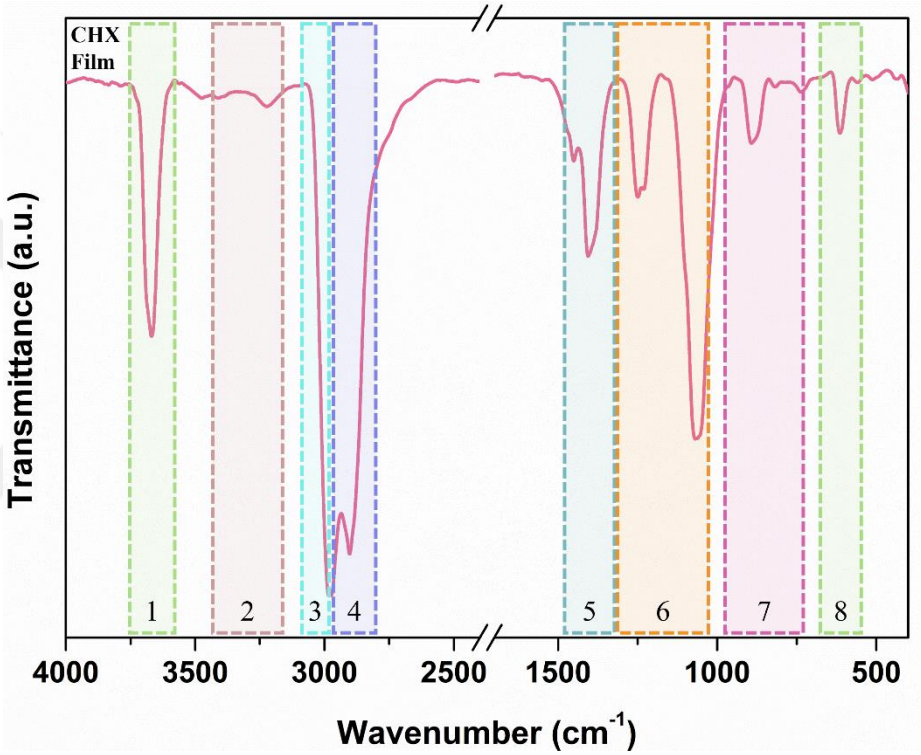

Figure 4.5 FTIR spectra of oCVD polymerized chlorhexidine thin film

Similarly, CHX thin films were too rinsed with methanol and the resultant FTIR image was depicted in the following Figure 4.6 As compared with the original thin film, methanol exposure didn't affect the chemical structure of the thin films instead the chemical bonds seem to be quite the same. Therefore (1) -OH bond between 3768 cm^{-1} – 3583 cm^{-1}, (2) Primary -N-H stretching between 3448 cm^{-1} – 3187 cm^{-1}, (3) Benzene ring between 3116 cm^{-1} – 2982 cm^{-1}, (4) -CH/-CH_2 stretching between 2973 cm^{-1} – 2823 cm^{-1}, (5) -C=C- aromatic ring between 1526 cm^{-1} – 1332 cm^{-1}, (6) -C-N and C-C overlapped stretching vibration between 1309 cm^{-1} – 983 cm^{-1}, and finally (7) -C-Cl stretching

between 940 cm^{-1} – 737 cm^{-1}, (8) -C-H stretching between 667 cm^{-1} – 555 cm^{-1} (Bettencourt et al., 2023; Onnainty et al., 2016; Pavia et al., 2015; Priyadarshini et al., 2017; Stuart & ProQuest, 2004; Yang et al., 2007).

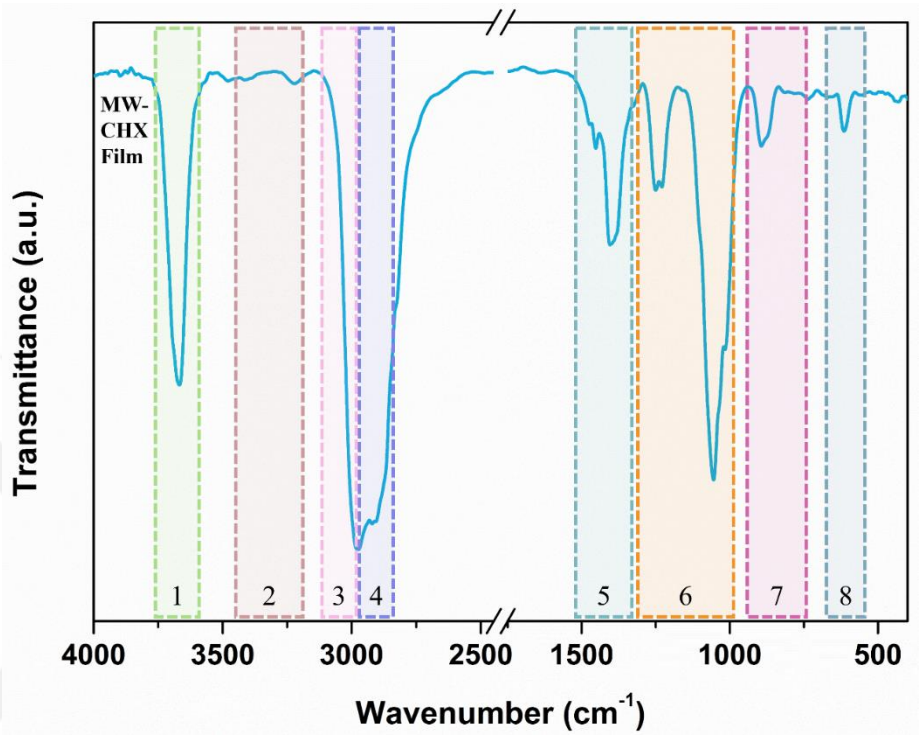

Figure 4.6 FTIR spectra of methanol rinsed chlorhexidine thin film

The final part of FTIR analysis completed with the analysis of the copolymer thin films. In the following Figure 4.7 CHX-TCS thin film has been demonstrated. The copolymerization process was completed in the same conditions which were under 100mTorr base pressure, vaporized TCS monomer at 125°C and CHX monomer at 165°C, when both monomers' vapor was sent to the reactor the pressure level was increased to 40mTorr, the reactor chamber was heated 50°C and the $FeCl_3$ oxidant was heated to 250°C. The polymerization took place for two hours.

When Figure 4.7 is analysed, all the peaks that were seen in the previous film were also visualized on the copolymer films. When the chemical bonds were revised respectively, (1) -OH bond was seen between 3512 cm^{-1} – 3304 cm^{-1}, (2) Primary -NH stretching between 3304 cm^{-1} – 3202 cm^{-1}, (3) Benzene ring between 3202 cm^{-1} – 2993 cm^{-1}, (4) -

CH/-CH_2 stretching between 2993 cm^{-1} – 2767 cm^{-1}, (5) -C=N stretching between 1672 cm^{-1} – 1579 cm^{-1}, (6) -C=C aromatic ring vibration between 1579 cm^{-1} – 1321 cm^{-1}, (7) -C-O-C- stretching vibration between 1115 cm^{-1} – 974 cm^{-1}, (8) -C-Cl stretching between 974 cm^{-1} – 754 cm^{-1}, and finally (9) -C-H vibration between 737 cm^{-1} – 605 cm^{-1}.

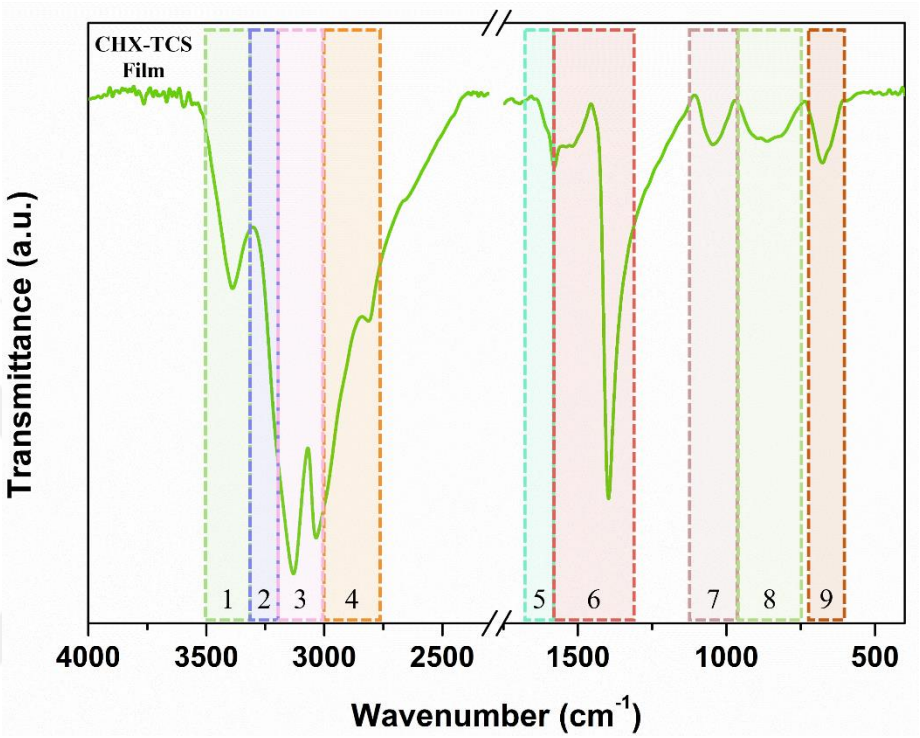

Figure 4.7 FTIR spectra of chlorhexidine & triclosan copolymer thin film

From the figure above, the polymerization process said to have taken place mostly from -C=N, C-N, C-C bonds since both lowered transmittance levels with low detection on the spectrum indicate the differences compared to monomers. So, in the film structure -C-Cl bond seems to be preserved this is quite notable since chlorine molecules interact with bacteria therefore it contributes to the antimicrobial activity of the films.

As for the previous films, copolymerized CHX-TCS thin films were also rinsed with methanol and the resultant graph has been demonstrated in Figure 4.8.

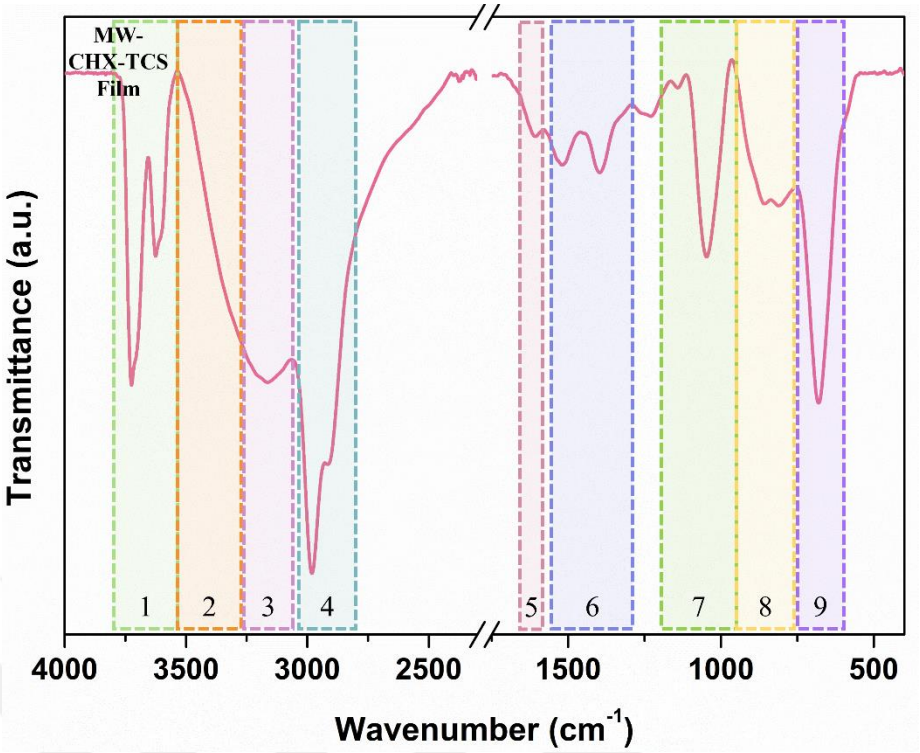

Figure 4.8 FTIR spectra of methanol rinsed chlorhexidine & triclosan thin film

As seen in the Figure 4.9, -NH bond and benzene ring peaks seem to be merged which might be related to methanol interaction. Additionally, aromatic ring peaks C=C bonds had a reduction in the transmittance level this might be related to the removal of unbounded monomer molecules from surfaces. Yet, the C-H bond seems to increase in terms of transmittance. When chemical bonds have been analysed respectively, (1) -OH bond was seen between 3773 cm^{-1} – 3537 cm^{-1}, (2) -NH stretching between 3537 cm^{-1} – 3316 cm^{-1}, (3) Benzene ring between 3316 cm^{-1} – 3043 cm^{-1}, (4) $-CH_3$/$-CH_2$ stretching between 3034 cm^{-1} – 2761 cm^{-1}, (5) -C=N stretching between 1655 cm^{-1} – 1576 cm^{-1}, (6) -C=C aromatic ring vibration between 1562 cm^{-1} – 1294 cm^{-1}, (7) -C-O-C- stretching vibration between 1188 cm^{-1} – 948 cm^{-1}, (8) -C-Cl stretching between 948 cm^{-1} – 754 cm^{-1}, and finally (9) -C-O-C vibration between 749 cm^{-1} – 599ss cm^{-1}.

For better understanding, both films were demonstrated in the following Figure 4.9

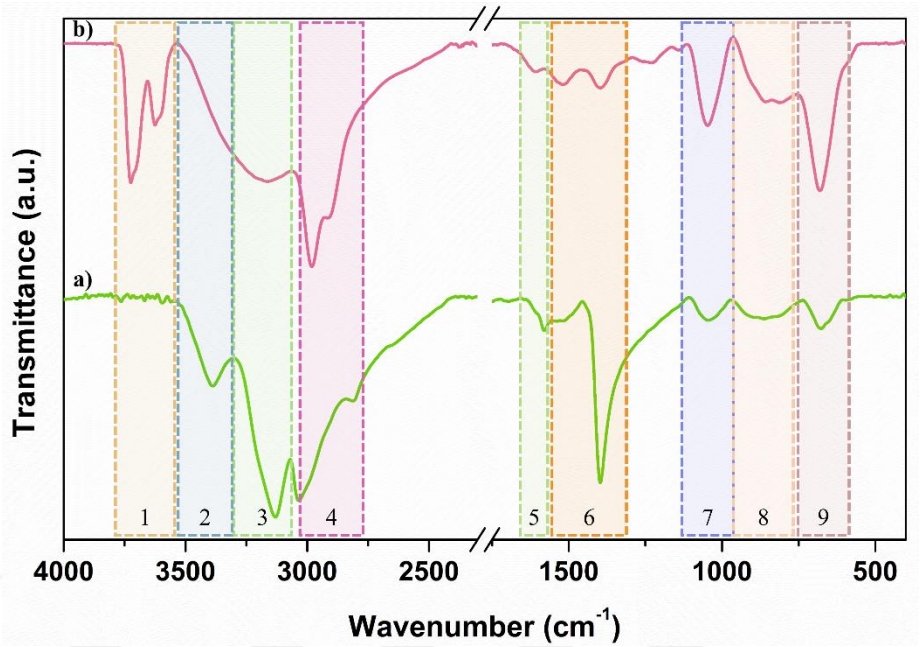

Figure 4.9 FTIR spectra comparison of a) CHX – TCS thin film, b) Methanol rinsed film

4.1.2 UV-vis analysis

In the analysis, firstly chemicals before thin film synthesis were screened. Following the polymerizations FTIR scans of samples have been taken from both glass slide samples and samples washed with methanol. UV-Vis scans were demonstrated with their corresponding monomers and methanol-rinsed thin films.

The first scan is all the triclosan samples in Figure 4.19 (a), monomer had a characteristic peak around 300-310 nm this comes from conjugated double bonds of the benzene ring and π-π* bond. In Figure 4.19 (b), two main peaks stand out at 325 nm and 380 nm they correspond to the conjugation of the monomer. The formation of dual peaks suggests interactions between polymer chains or possible oxidation-induced structural changes. Lastly, in Figure 4.19 (c), there seems a change has taken place in the structure. One of the main reasons could be removal of unreacted monomer molecules from the surface. The long extension of the line proves the long polymeric structure of the thin film with its rough morphology.

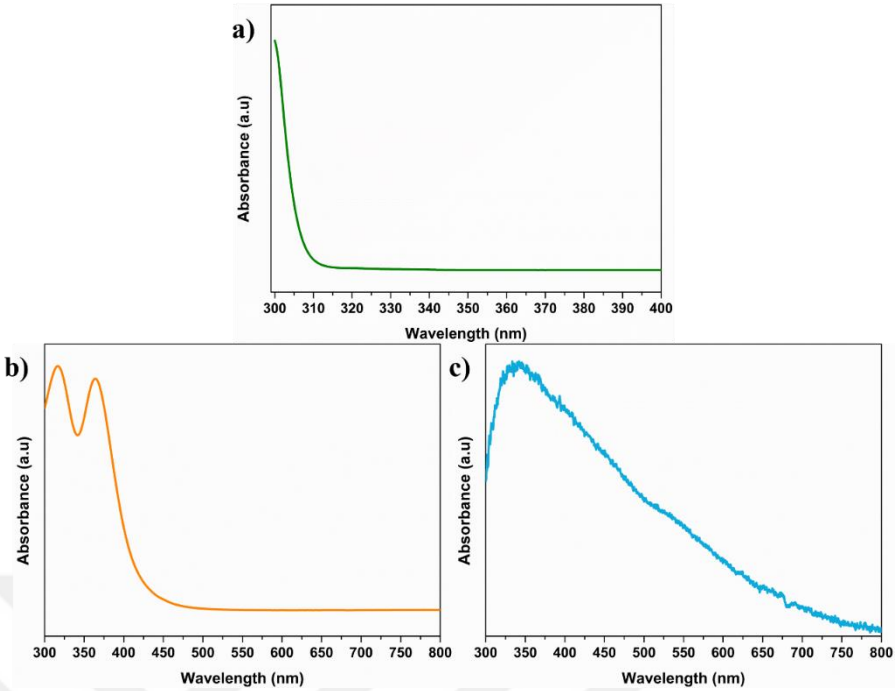

Figure 4.10 UV-Vis spectra of a) triclosan monomer, b) triclosan thin film and c)methanol rinsed triclosan thin film

In the following Figure 4.20 (a), the CHX monomer demonstrates a smooth absorption line which is related to the benzene ring and the transition of π-π* bond. In Figure 4.20 (b), The changes between 300 – 450 nm indicate that during polymerization the structure of the monomer vary reorder itself. Similar to TCS, in CHX films extended chain (red-shift) formation during polymerization was observed. For the methanol rinsed sample in Figure 4.20 (c), unreacted monomeric residues have been said to be removed from the surface. Rinsing with the methanol didn't have a major differentiating effect on the surface instead polymer chains seem to keep untouched.

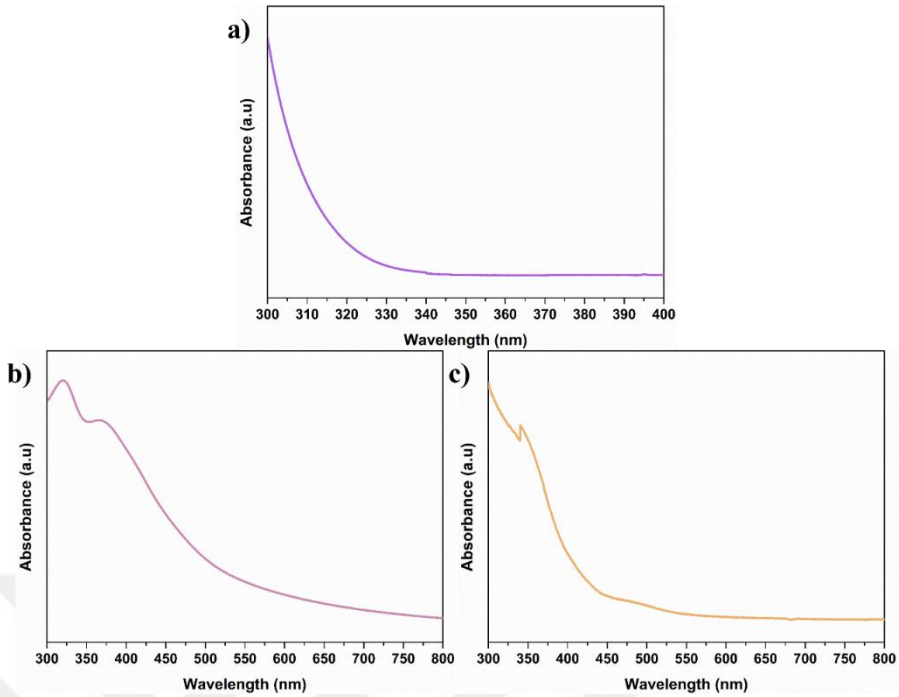

Figure 4.11 UV-Vis spectra of a) chlorhexidine monomer, b) chlorhexidine thin film and c)methanol rinsed chlorhexidine thin film

In Figure 4.21 (a), the broadened spectrum demonstrates the copolymerization between triclosan and chlorhexidine therefore polymer chain reaction. On the methanol rinsed graph (Figure 4.21 (b)), reduced absorption peaks correspond to the removal of loosely bounded polymer chains.

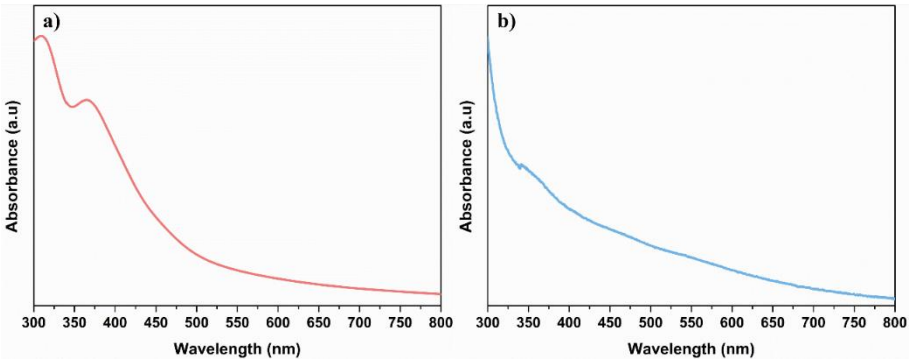

Figure 4.12 UV-Vis spectra of a) chlorhexidine-triclosan thin film, b) methanol rinsed chlorhexidine-triclosan thin film

4.1.3 XPS analysis

XPS analysis was made in 'depth profile' mode where the scans were taken from the successive layer under high vacuum conditions. In the XPS deconvolution analysis, the R^2 value had been stabilized around 0.92 to reach maximum data fitting. In the first part, triclosan polymer has been detailed with C1s, O1s, Cl2p and Fe2p spectrum deconvolution graphs and associated details of the atomic percentages have been detailed in the tables.

The chemical bonds seen in the deconvolution graphs had a direct correlation with the FTIR graph. Figure 4.12 a is the C1s spectrum and in the deconvolution peaks C=C and C-C peaks had a great abundance, this is because the majority of the aromatic ring didn't break during polymerization instead, they made a bond from C-Cl bond. As compared with the FTIR spectrum, in the C-Cl bond has not been detected since the majority of the bonds have been broken. However, the depth analysis of XPS showed that during polymerization a part of triclosan monomers didn't lose their -Cl molecules. This was important for enhancing antimicrobial activity since it causes changes in bacterial membrane permeability which is directly related to the inhibition of bacteria. The presence of -Cl ions can be due to both the structural composition of triclosan and oxidative agent. In the Figure 4.12 d Fe^{2+} and Fe^{3+} ions have appeared in the depth analysis. The presence of such ions implies that during methanol wash, sample surfaces were not fully purified from oxidative species. As a result, related peaks have appeared on the XPS scans.

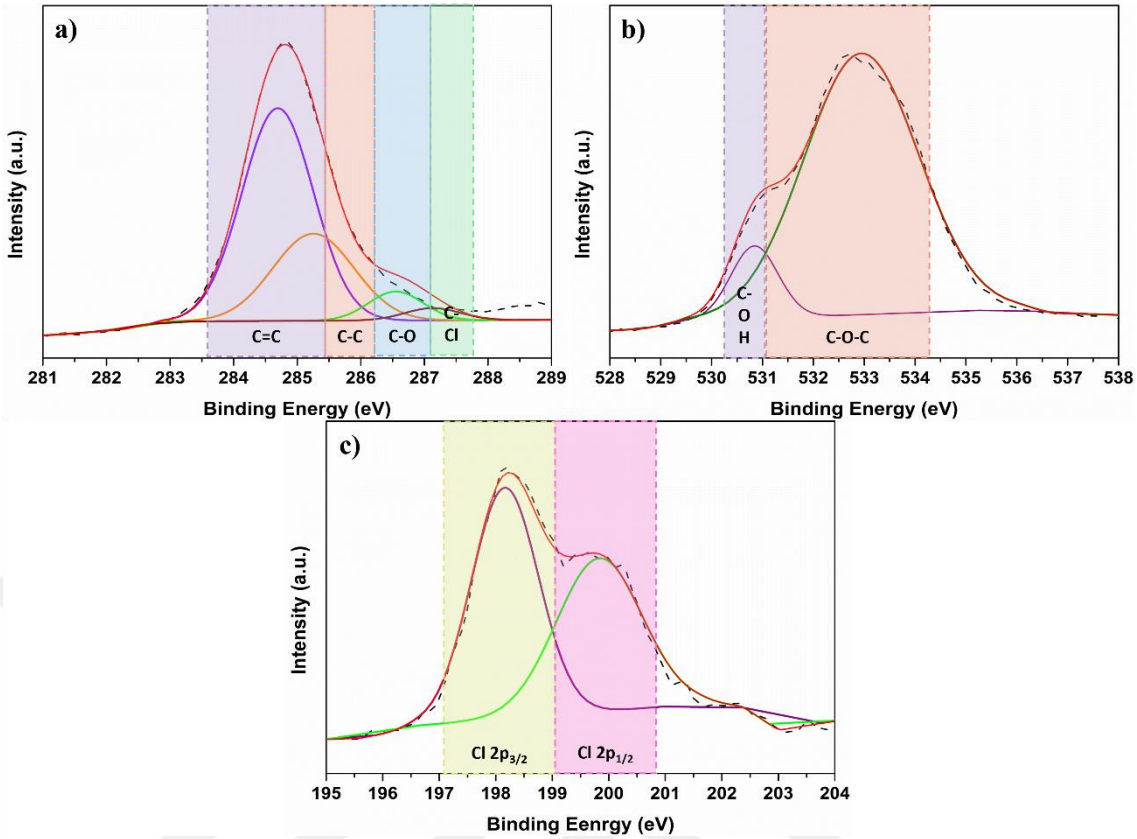

Figure 4.13 XPS spectra of TCS thin film. The deconvolution of chemicals bonds has been demonstrated in the following order, a) C1s spectra, b) O1s spectra, c)Cl2p spectra

Table 4.1 C1s deconvolution parameters of the TCS thin films (Beamson, 1992)

TCS C1s Spectra			
Bonds	**Center Max**	**FWHM**	**Area %**
C=C / Benzene Ring	284.69	1.32	62.00
C-C	285.25	1.50	28.79
C-O	286.55	1.01	6.42
C-Cl	287.13	1.03	2.78

Table 4.2 O1s deconvolution parameters of the TCS thin films (Beamson, 1992)

TCS O1s Spectra			
Bonds	**Center Max**	**FWHM**	**Area %**
-OH	530.84	1.09	10.25
C-O-C	532.94	2.65	89.74

Table 4.3 Cl2p deconvolution parameters of the TCS thin films (Beamson, 1992)

TCS Cl2p Spectra			
Bonds	**Center Max**	**FWHM**	**Area %**
Cl $2p_{3/2}$	198.16	1.40233	54.18862
Cl $2p_{1/2}$	199.82901	1.78788	45.81138

The following graphs are depth profiles of chlorhexidine thin films. Similar to triclosan, chlorhexidine thin films correlated FTIR spectra too. From the spectra, both C=C and C-C bonds had a great majority as seen from Figure 4.13 a, differently from triclosan C-Cl bonds had a higher presence this is because during polymerization mainly took place from C-N and C=N bonds. Similar to triclosan, Fe^{2+} and Fe^{3+} ions were also detected in chlorhexidine films.

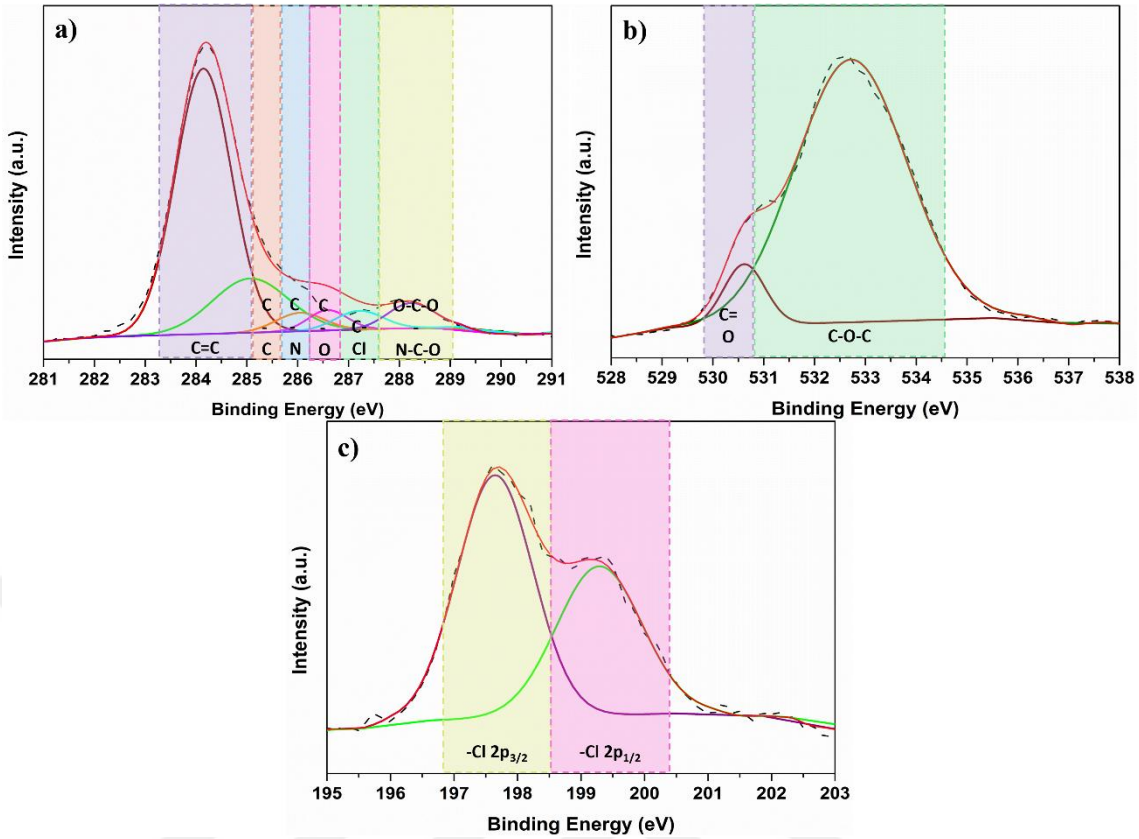

Figure 4.14 XPS spectra of CHX thin film. Deconvolution of chemical bonds have been demonstrated in the following order, a) C1s spectra, b) O1s spectra, c) Cl2p spectra

Table 4.4 C1s deconvolution parameters of the CHX thin films

(Beamson, 1992; Sodhi et al., 1992)

CHX C1s Spectra			
Bonds	**Center Max**	**FWHM**	**Area %**
C=C / Benzene Ring	284.15	1.30	65.46
C-C	285.07	1.76	18.03
C-N	286.05	1.12	3.91
C-O	286.59	0.91	3.51
C-Cl	287.21	1.10	3.92
N-C-O / O-C-O	288.23	1.08	5.17

Table 4.5 O1s deconvolution parameters of the CHX thin films

(Beamson, 1992; Sodhi et al., 1992)

CHX O1s Spectra			
Bonds	**Center Max**	**FWHM**	**Area %**
C=O	530.99	0.96	7.95
C-O-C	532.72	2.58	92.05

Table 4.6 Cl2p deconvolution parameters of the CHX thin films

(Beamson, 1992; Sodhi et al., 1992)

CHX Cl2p Spectra			
Bonds	**Center Max**	**FWHM**	**Area %**
Cl $2p_{3/2}$	197.65	1.41	59.17
Cl $2p_{1/2}$	199.29	1.59	40.83

The following XPS data were the graphs obtained from copolymer CHX-TCS thin film. Differently from triclosan and chlorhexidine spectra C=C and C-C bonds had lower deconvolution peaks seen in Figure 4.14 a. This was related to polymerization reaction between chemicals. Due to reactions the band presence of C-O-C and C-Cl bonds had lower percentages.

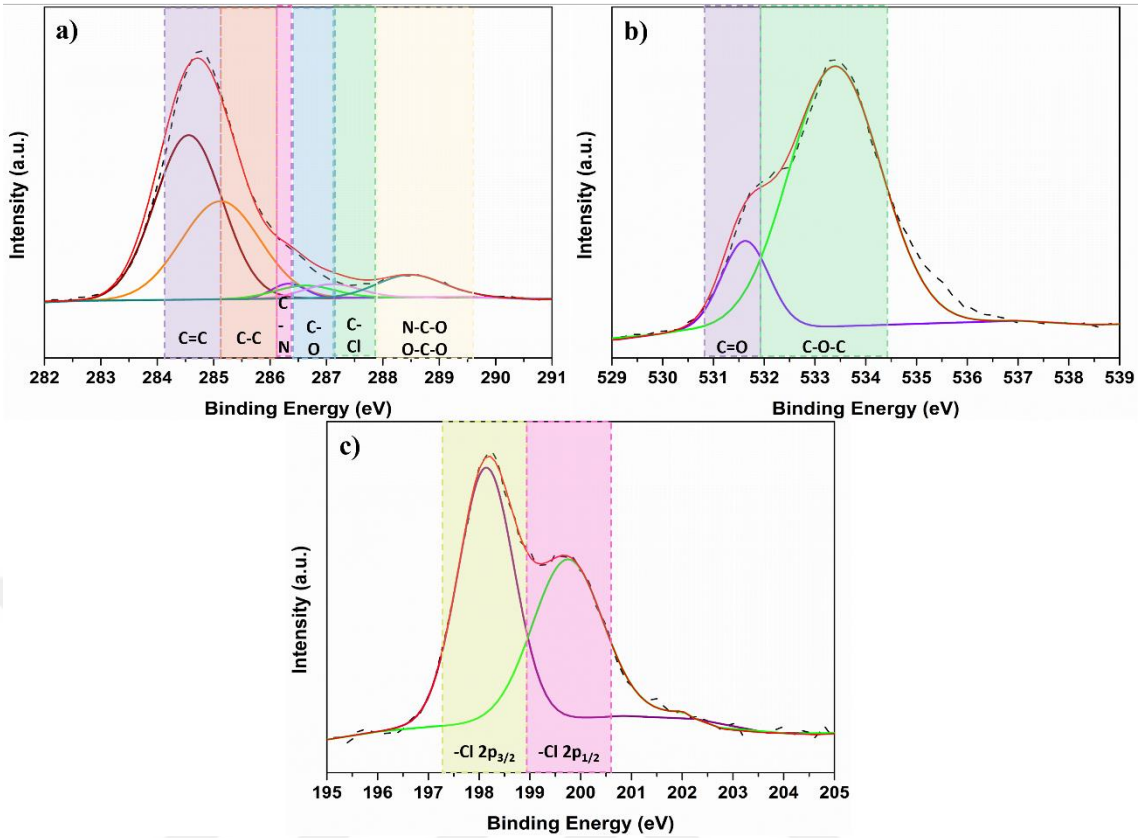

Figure 4.15 XPS spectra of CHX-TCS thin film. The deconvolution of chemical bonds have been demonstrated in the following order, a) C1s spectra, b) O1s spectra c) Cl2p spectra, d) N1s spectra and e) Fe2p spectra

Table 4.7 C1s deconvolution parameters of CHX-TCS thin films (Beamson, 1992)

CHX - TCS C1s XPS Spectra			
Bonds	**Center Max**	**FWHM**	**Area %**
C=C / Benzene Ring	284.55	1.39	49.50132
C-C	285.12	1.64	34.61215
C-N	286.32	0.71	2.27349
C-O	286.62	1.25	3.4451
C-Cl	287.09	1.17	3.52016
N-C-O/O-C-O	288.48	1.37	6.64778

Table 4.8 O1s deconvolution parameters of CHX-TCS thin films (Beamson, 1992)

CHX - TCS O1s Spectra			
Bonds	**Center Max**	**FWHM**	**Area %**
C=O	531.62	1.10	14.92
C-O-C	533.39	2.13	85.08

Table 4.9 Cl2p deconvolution parameters of CHX-TCS thin films (Beamson, 1992)

CHX –TCS Cl 2p Spectra			
Bonds	**Center Max**	**FWHM**	**Area %**
Cl $2p_{3/2}$	198.14	1.29	56.06
Cl $2p_{1/2}$	199.74	1.63	43.94

4.1.4 SEM analysis

SEM images were taken from methanol rinsed samples, and images were visualized between 200x, 500x, 1000x, 2000x, 5000x and 10000x magnifications. In the first image thin film of triclosan has been demonstrated. From images, it seems that by time triclosan coatings lose their uniformity and minor scale cracks start to form on the surfaces. Crack initiation can also be related to dehydrated storage conditions and methanol rinsing.

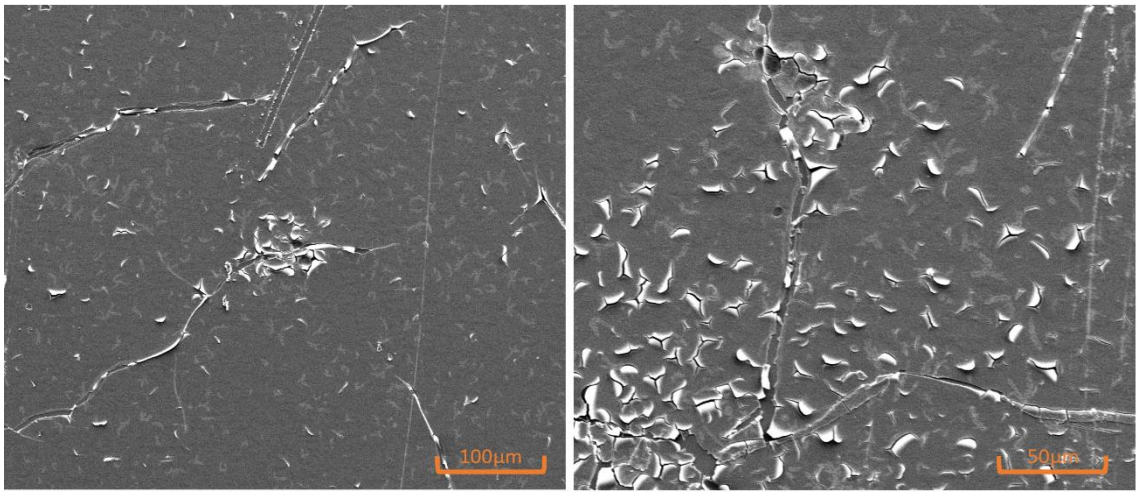

Figure 4.16 SEM image of TCS thin film

The following image is the SEM scan of chlorhexidine thin film. Contrary to triclosan, chlorhexidine had better uniformity on surfaces and any crack formation didn't seem to happen. As magnification increased certain repetitive shapes/entities became visible on the images. During polymerization excited monomer molecules could pile on each other and constant monomer vapor flow clumps and irregularly shaped entities seem to form. Another reason for such formation can also be related to the post-polymerization interaction between polymer chains and monomer vapor.

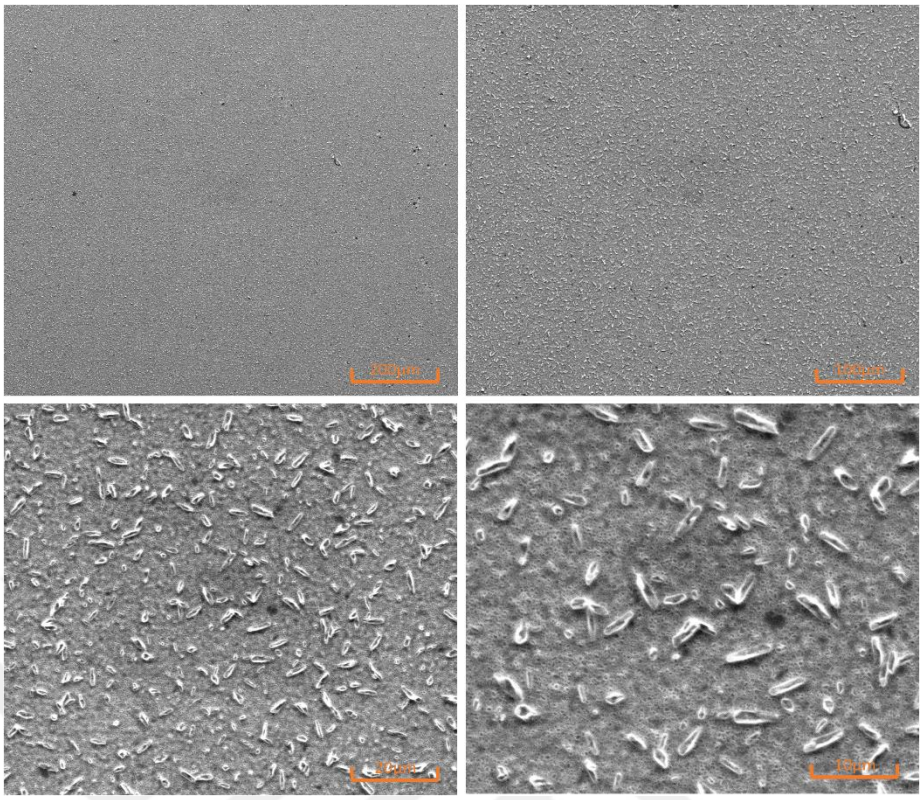

Figure 4.17 SEM image of CHX thin film

The following SEM image is the copolymerized CHX-TCS thin film. As seen from the image, the interaction between TCS and CHX formed a thin film with a similar structure to the previous thin film. Similar to CHX thin film, surfaces had homogenous coatings and small entities formed on the surfaces. Differently from previous films, copolymer films had better evenness with smaller size entities.

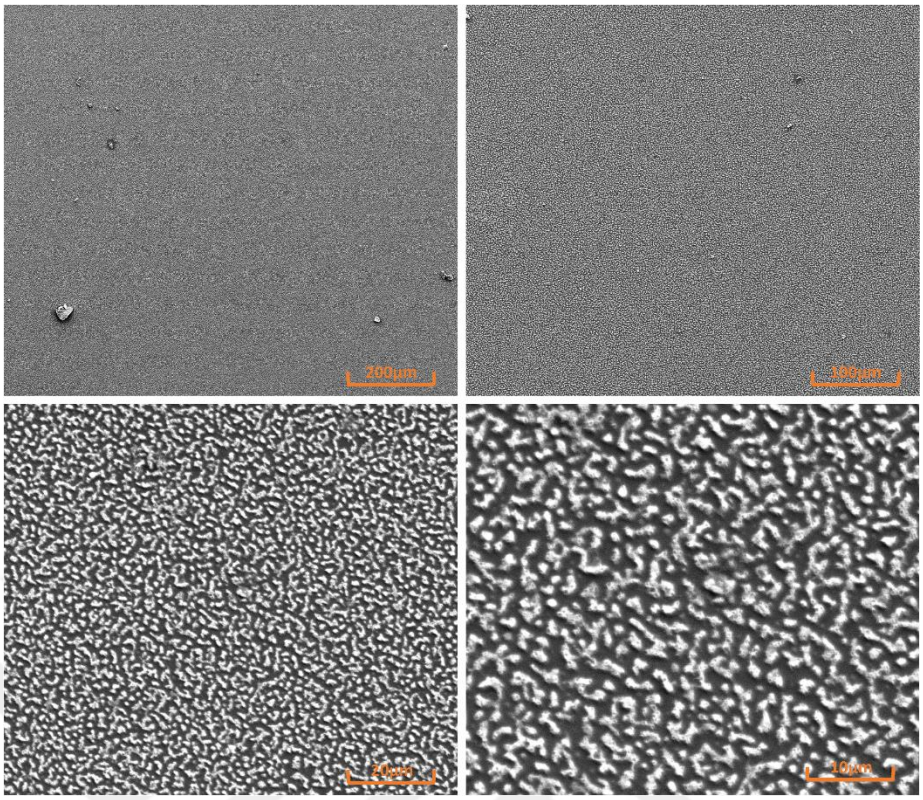

Figure 4.18 SEM image of CHX-TCS thin film

4.2 Microbiological Analysis

Microbiology studies were carried out during four different periods for the sake of testing long term effectiveness of the coatings. Similar to FTIR analysis, TCS and CHX thin films were also tested against each bacteria for comparison with copolymer thin films. In the following figures, each pair of graphs is composed of the ones where the bacteria were able to adhere on gutta percha surfaces and the ones that where able to remain alive on the feedlot respectively. So, for each graph, the ones on the left-hand side account for the surface adherent bacteria and the right-hand side was the surviving bacteria on the feedlot. For each graph, results were compared with the uncoated catheter incubations, in this way inhibitor effect of the coatings was compared.

When coated gutta percha samples were incubated with *S.epidermidis* suspension, all types of them had quite high inhibition rates throughout the incubation period. For TCS-FeCl3 coating inhibition rates of the bacteria which were adhered on the gutta percha surface and the ones unable to hold yet survived in the feedlot respectively varied from

94.9% to 99.2%. As seen from the following figures, coated surfaces had quite low bacterial colonies on the surfaces.

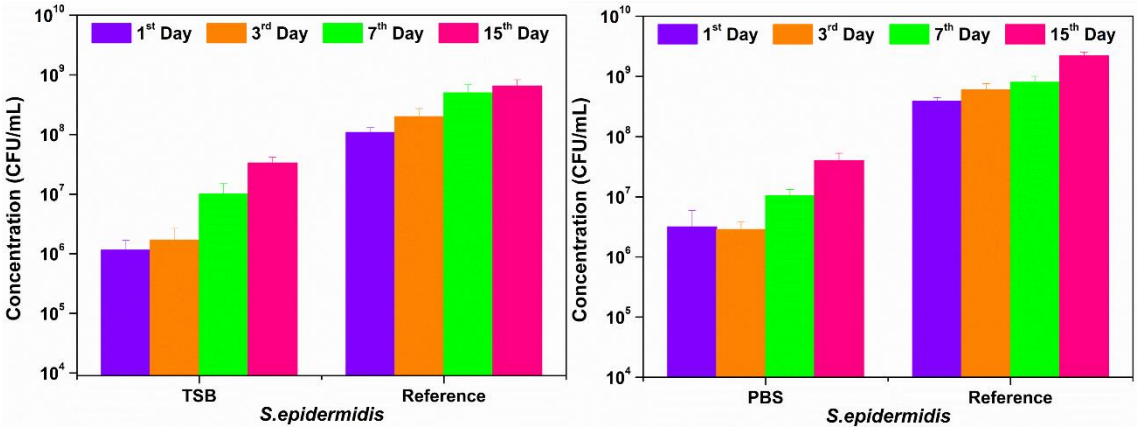

Figure 4.19 Colony numbers of *S.epidermidis* that was able to adsorb on gutta percha surfaces coated with TCS thin films and the ones were remained alive on the feedlot

For the methanol rinsed samples, inhibition rates were comparably lower as rates varied between 77.5% to 98.5%. As it's clear from the following figure, even though the coatings were able to eliminate adherence of bacteria yet, it wasn't enough to inhibit the ones on the feedlot. It might be related to the interaction between methanol and coatings. Since, methanol might have removed a great majority of the coatings from gutta percha surfaces and this caused slightly reduced inhibition effect of coatings.

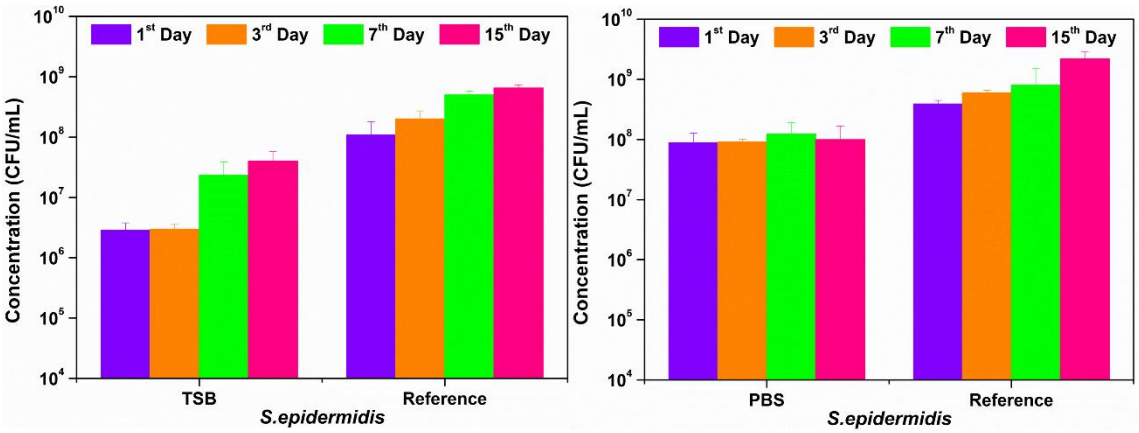

Figure 4.20 Colony numbers of *S.epidermidis* that was able to adsorb on gutta percha surfaces which were methanol rinsed following the TCS polymerization and the ones were remained alive on the feedlot.

The following figure demonstrates the inhibitor effect of chlorhexidine against *S.epidermidis* contrary to triclosan, chlorhexidine demonstrated superior inhibition. This is because the inhibition rates have varied from 88% to 99.6% for adhered bacteria. For the feedlot surviving bacteria, inhibition rates have varied between 80.2% to 99.8%. This difference in the inhibition might be related to strong adherence to chlorhexidine coating on the gutta percha surfaces. Because, strong covalent bonding between coatings and gutta percha surfaces might restrain the diffusion of antimicrobial agents from the surfaces. Therefore, bacteria surviving on the feedlot preserved their presence. Even though inhibition rates for feedlot bacteria are lower than adhered bacteria coatings still preserved their antimicrobial activity.

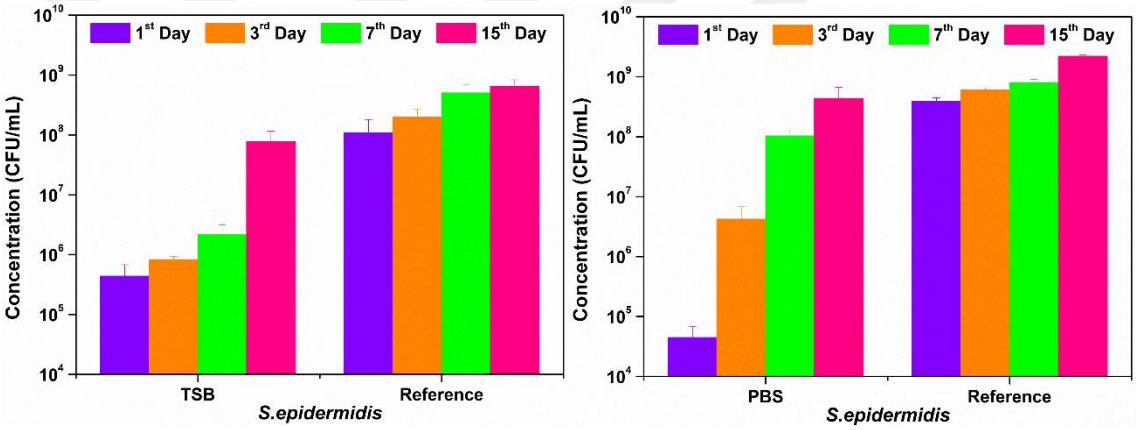

Figure 4.21 Colony numbers of *S.epidermidis* that was able to adsorb on gutta percha surfaces that were CHX coated and the ones were remained alive on the feedlot

Similar to triclosan, when chlorhexidine was rinsed with methanol inhibition rates got lower but still inhibition rates for the adhered bacteria varied between 79.6% to 99.0%. Likewise, the remaining bacteria in the feedlot were inhibited between 75.9% to 99.0%.

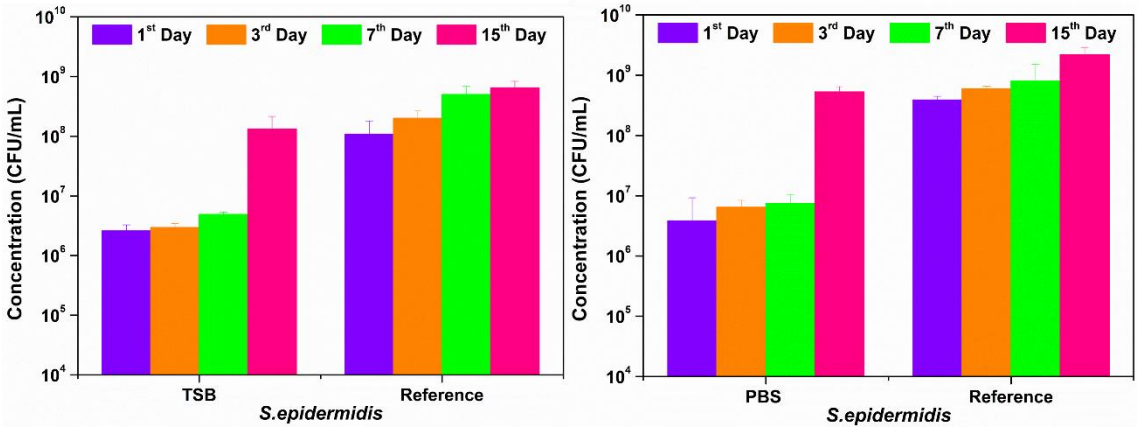

Figure 4.22 Colony numbers of *S.epidermidis* that was able to adsorb on gutta percha surfaces that were methanol rinsed following the CHX polymerization and the ones were remained alive on the feedlot

The following graph is a demonstration of the combination of triclosan and chlorhexidine. As seen from the graphs combined effect of triclosan and chlorhexidine had a superior effect as an inhibitor on the gutta perchas. As expected and intended at the beginning of the thesis studies when both antimicrobial agents were used together, their antimicrobial effects multiplied. For surface adhered bacteria inhibition rates were the highest among all the coatings. Ranging between 96.95 to 99.7%.

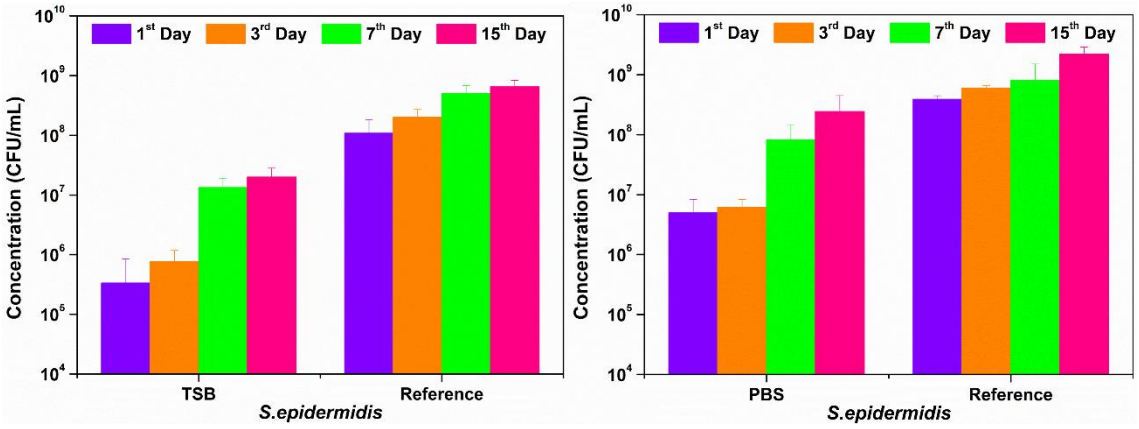

Figure 4.23 Colony numbers of *S.epidermidis* that was able to adsorb on gutta percha surfaces that were coated with CHX-TCS copolymer and the ones were the remained alive on the feedlot

Opposed to other methanol rinsed samples, CHX-TCS coatings preserved their antimicrobial activity even after rinsing.

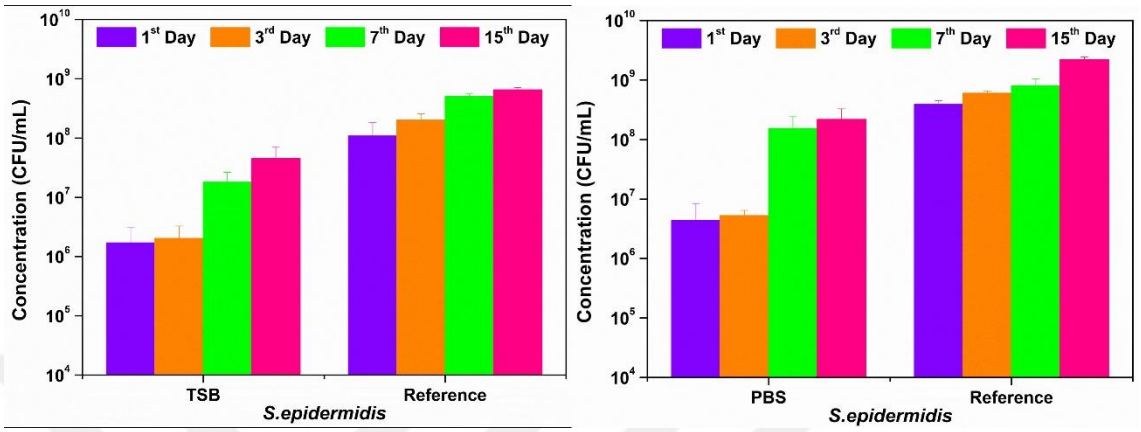

Figure 4.24 Colony numbers of *S.epidermidis* that was able to adsorb on gutta percha surfaces which were coated with methanol rinsed CHX-TCS copolymer and the ones were remained alive on the feedlot

When the antimicrobial activity of triclosan and chlorhexidine were analyzed against *E.coli* similar inhibiting activity was also achieved. For triclosan, inhibition rates varied between 95.5% to 99.6% for adhered bacteria, for feedlot surviving bacteria rates were quite similar which was between 95.4% to 98.2%.

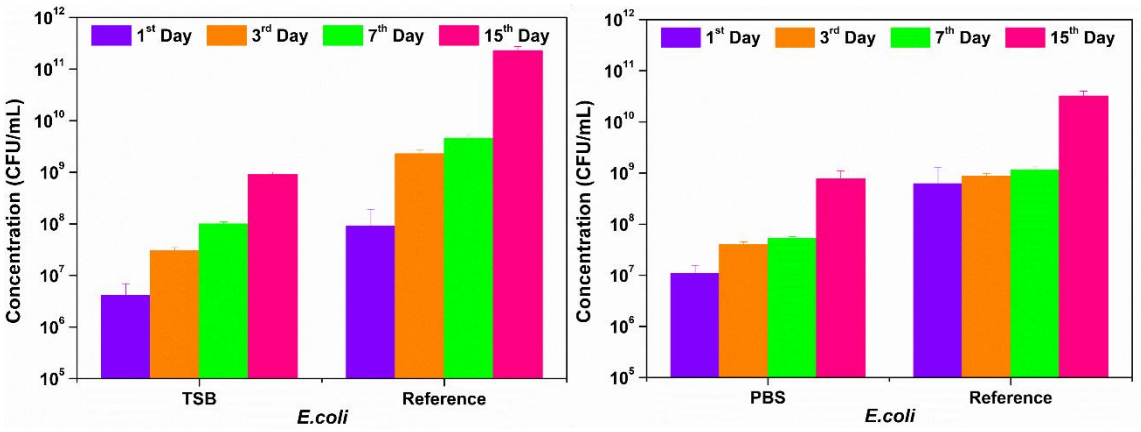

Figure 4.25 Colony numbers of *E.coli* that were able to adsorb on gutta percha surfaces coated with TCS thin films and the ones were remained alive on the feedlot

After methanol rinsing, contrary to *S.epidermidis*, *E.coli* was successfully eliminated with the inhibition rates varying between 91.3% to 99.7%.

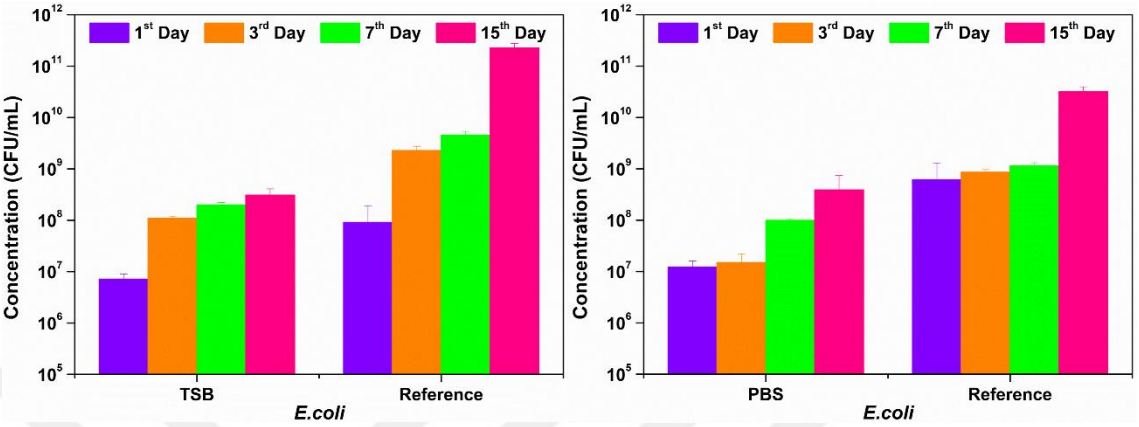

Figure 4.26 Colony numbers of *E.coli* that were able to adsorb on gutta percha surfaces which that methanol rinsed following the TCS polymerization and the ones were remained alive on the feedlot

Similar to *S.epidermidis, E.coli* was also successfully eliminated with the use of chlorhexidine both from gutta percha surfaces and from feedlot. Inhibition rates were 92.7% to 99.9% and 69.8% to 99.2% respectively.

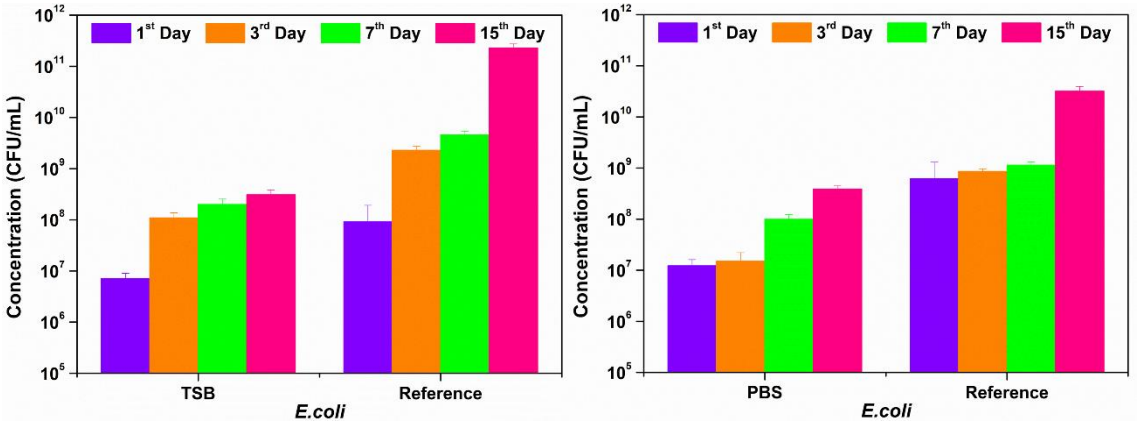

Figure 4.27 Colony numbers of *E.coli* that was able to adsorb on gutta percha surfaces that were CHX coated and the ones were remained alive on the feedlot

Opposed to *S.epidermidis*, methanol rinsing didn't cause a significant reduction in the inhibition levels. For the adhered bacteria inhibition rates varied between 93.3% to 99.8% and for the remaining ones 61.3% to 99.9%.

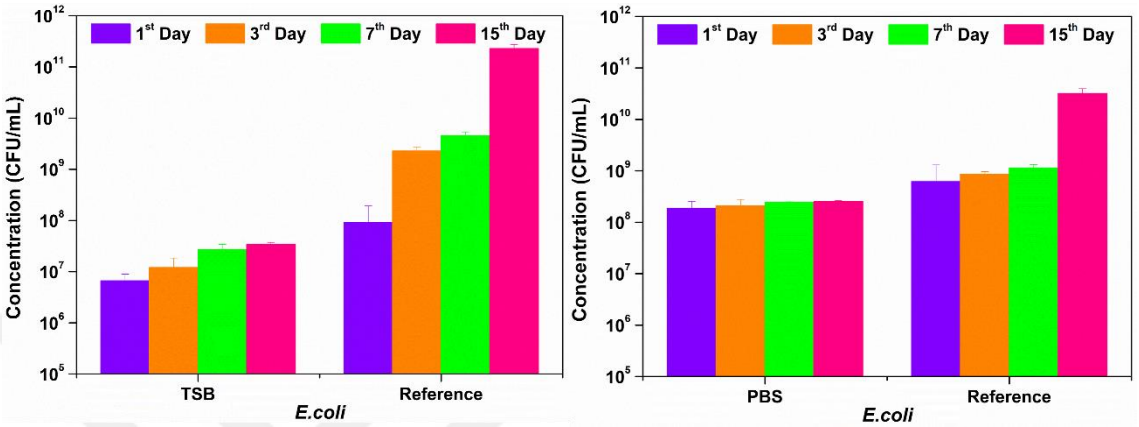

Figure 4.28 Colony numbers of *E.coli* that were able to adsorb on gutta percha surfaces which were methanol rinsed following the CHX polymerization and the ones remained alive on the feedlot

As aimed combination of triclosan and chlorhexidine improved their antimicrobial activity. Inhibition rates were increased to 88.6% to 99.9% for adhered bacteria and 86.8% to 99.3% for the remaining bacteria.

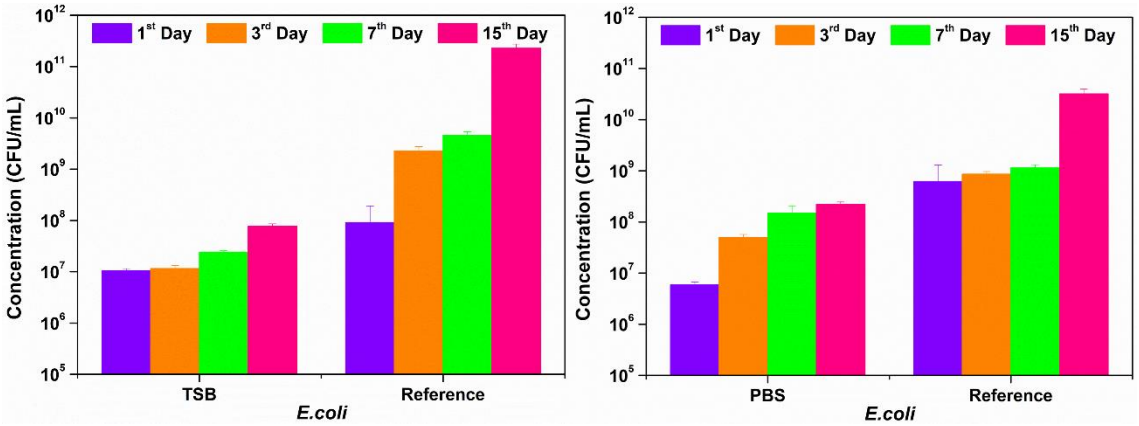

Figure 4.29 Colony numbers of *E.coli* that were able to adsorb on gutta percha surfaces that were coated with CHX-TCS copolymer and the ones were remained alive on the feedlot

Similar successful inhibition effects were achieved even after methanol rinsing with 91.4% to 99.9% for adhered and 87.0% to 99.3% remaining ones.

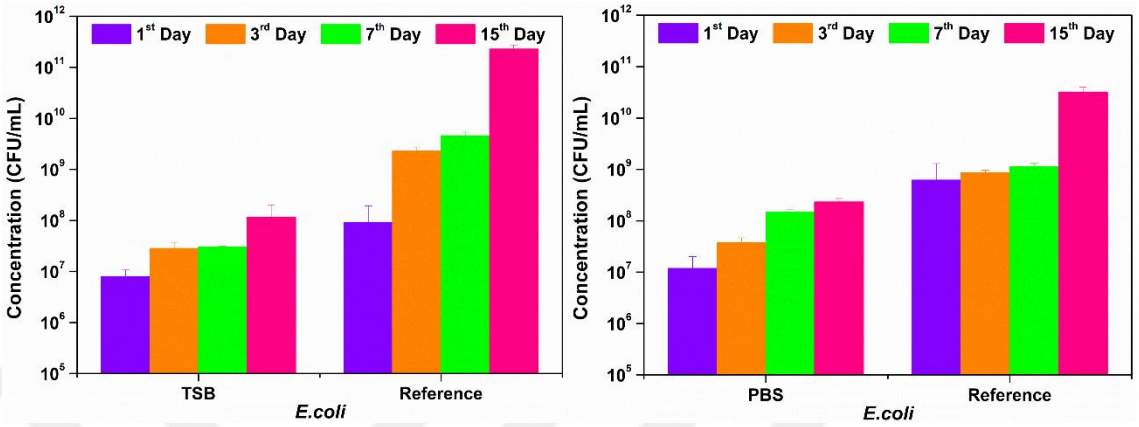

Figure 4.30 Colony numbers of *S.epidermidis* that was able to adsorb on gutta percha surfaces that were coated with methanol rinsed CHX-TCS copolymer and the ones were remained alive on the feedlot

As bacterial incubation results have shown, even though both of the monomers had antimicrobial activity against both bacteria their combination had a surpassing effect. With such results, it can be said that coatings provide antimicrobial activity and can be applied to other medical device surfaces.

Table 4.10 % Inhibition rates of Triclosan and $FeCl_3$ on *E.coli* and *S.epidermidis*

TCS & FeCl3							
E.coli - TSB				***E.coli - PBS***			
1st Day	**3rd Day**	**7th Day**	**15th Day**	**1st Day**	**3rd Day**	**7th Day**	**15th Day**
95.4883	98.6875	97.8125	99.6063	98.2419	95.3642	95.4386	97.6094
S.epidermidis - TSB				***S.epidermidis - PBS***			
1st Day	**3rd Day**	**7th Day**	**15th Day**	**1st Day**	**3rd Day**	**7th Day**	**15th Day**
98.9436	99.15	98	94.8718	99.188	99.5222	98.7083	98.1818

Table 4.11 % Inhibition rates of Methanol Washed Triclosan and $FeCl_3$ on *E.coli* and *S.epidermidis*

TCS & FeCl3 - Methanol Washed							
E.coli - TSB				***E.coli - PBS***			
1st Day	**3rd Day**	**7th Day**	**15th Day**	**1st Day**	**3rd Day**	**7th Day**	**15th Day**
92.1615	95.1875	95.625	99.8644	98.0242	98.2616	91.2281	98.7813
S.epidermidis - TSB				***S.epidermidis - PBS***			
1st Day	**3rd Day**	**7th Day**	**15th Day**	**1st Day**	**3rd Day**	**7th Day**	**15th Day**
97.3622	98.5167	95.3333	93.8462	77.5299	84.8722	84.5834	95.4545

Table 4.12 % Inhibition rates of Chlorhexidine and $FeCl_3$ on *E.coli* and *S. epidermidis*

CHX & FeCl3							
E.coli - TSB				***E.coli - PBS***			
1st Day	**3rd Day**	**7th Day**	**15th Day**	**1st Day**	**3rd Day**	**7th Day**	**15th Day**
92.7266	99.475	99.4167	99.9851	69.6774	75.6623	78.7719	99.2109
S.epidermidis - TSB				***S.epidermidis - PBS***			
1st Day	**3rd Day**	**7th Day**	**15th Day**	**1st Day**	**3rd Day**	**7th Day**	**15th Day**
97.3622	98.5167	95.3333	93.8462	77.5299	84.8722	84.5834	95.4545

Table 4.13 % Inhibition rates of Methanol Washed Chlorhexidine and $FeCl_3$ on *E.coli* and *S.epidermidis*

CHX & FeCl3 - Methanol Washed							
E.coli - TSB				***E.coli - PBS***			
1st Day	**3rd Day**	**7th Day**	**15th Day**	**1st Day**	**3rd Day**	**7th Day**	**15th Day**
93.3464	99.7521	98.0313	99.4689	97.9032	4.38742	61.2573	99.8688
S.epidermidis - TSB				***S.epidermidis - PBS***			
1st Day	**3rd Day**	**7th Day**	**15th Day**	**1st Day**	**3rd Day**	**7th Day**	**15th Day**
97.6075	98.525	99.02	79.6154	99.0128	98.9208	99.0688	75.9091

Table 4.14 % Inhibition rates of Chlorhexidine – Triclosan and $FeCl_3$ on *E.coli* and *S.epidermidis*

CHX & TCS & FeCl3							
E.coli - TSB				***E.coli - PBS***			
1st Day	**3rd Day**	**7th Day**	**15th Day**	**1st Day**	**3rd Day**	**7th Day**	**15th Day**
88.625	99.4947	99.475	99.9665	99.0511	94.2459	86.8421	99.3063
S.epidermidis - TSB				***S.epidermidis - PBS***			
1st Day	**3rd Day**	**7th Day**	**15th Day**	**1st Day**	**3rd Day**	**7th Day**	**15th Day**
99.6929	99.62	97.3333	96.9231	98.7231	98.97	89.75	88.9091

Table 4.15 % Inhibition rates of Methanol Washed Chlorhexidine – Triclosan and $FeCl_3$ on *E.coli* and *S.epidermidis*

CHX & TCS & FeCl3 - Methanol Washed							
E.coli - TSB				***E.coli - PBS***			
1st Day	**3rd Day**	**7th Day**	**15th Day**	**1st Day**	**3rd Day**	**7th Day**	**15th Day**
91.4469	98.7641	99.3438	99.9493	98.0968	95.6829	87.0175	99.2708
S.epidermidis - TSB				***S.epidermidis- PBS***			
1st Day	**3rd Day**	**7th Day**	**15th Day**	**1st Day**	**3rd Day**	**7th Day**	**15th Day**
98.4357	98.99	96.4	93.0769	98.8782	99.1233	80.9375	90.0909

4.3 Zone of Inhibition Analysis

The following inhibition zone results have been acquired at different periods of time to see the long-term antibacterial activity of the coatings. In the first section, uncoated gutta perchas were incubated with *E.coli* and *S.epidermidis* bacterial cultures at the same periods with the coatings. As seen from Figure 4.45 And Figure 4.46, uncoated gutta percha's were unable to eliminate bacteria from either their surfaces or from a smaller area. Throughout the analysis period, agar plates tend to dry up therefore on the figures the ones closer to the 15^{th} day had cracks and colour changes on the surfaces.

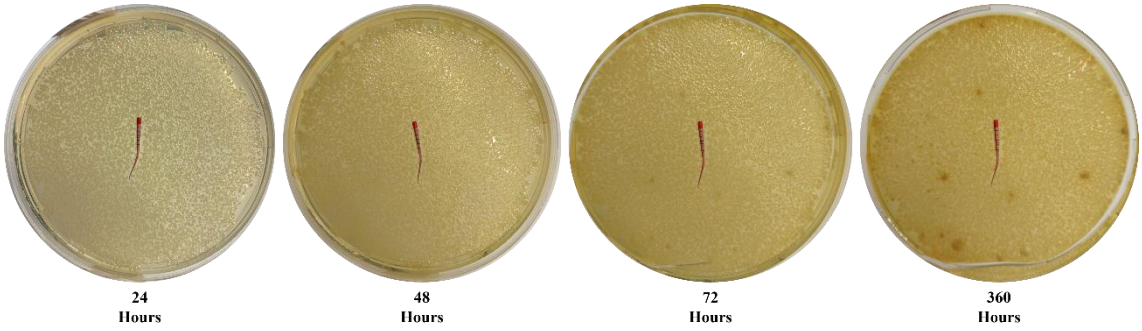

Figure 4.31 Agar plates of control gutta perchas with *E.coli* during the Inhibition Zone Test incubation on different days

Figure 4.32 Agar plates of control gutta perchas with *S.epidermidis* during Inhibition Zone Test incubation on different days

The following images are thin film coated gutta percha samples, from the resultant images it was concluded that triclosan alone had limited effectiveness against *E.coli*. Even though on the first day gutta percha had a protective layer around the tip area, it slowly disappeared up to the 15th day. The resistance of *E.coli* against triclosan was published by different articles (Li et al., 2019; Zeng et al., 2020). The known reason for this phenomenon is related to the interaction between TCS and *E.coli*. As TCS molecules interact with the environment it causes the formation of oxidative species and the reaction with *E.coli* causes a stimulation that leads to mutations in the cell membrane integrity cascade (Lu et al., 2018). Therefore, over time *E.coli* develops resistance to certain chemicals such as triclosan.

Figure 4.33 Agar plates of TCS-$FeCl_3$ Methanol Washed *E.coli* samples

As the control group, CHX-$FeCl_3$ Methanol Washed and CHX-$FeCl_3$ coated gutta perchas were also incubated with *E.coli*. From the images as opposed to the expected results, chlorhexidine didn't have an effective inhibition effect against *E.coli*. One of the main reasons for such a result may be related to the non-diffusing characteristic of chlorhexidine coating or in other words, limited/inadequate release of coatings. If insufficient chlorhexidine reacts with *E.coli*, it might not be able to inhibit metabolic activities and therefore unable to inhibit bacterial proliferation. Another possible reason could be similar to inadequate release of antimicrobial agent release from the coatings.

Figure 4.34 Agar plates of CHX-$FeCl_3$ Methanol Washed *E.coli* samples

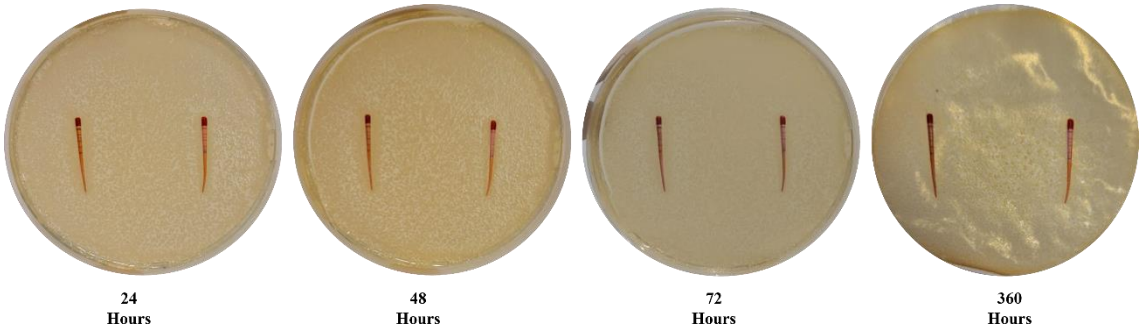

Figure 4.35 Agar plates of CHX-$FeCl_3$ *E.coli* samples

Figure 4.36 Agar plates of CHX-TCS-$FeCl_3$ Methanol Washed *E.coli* samples

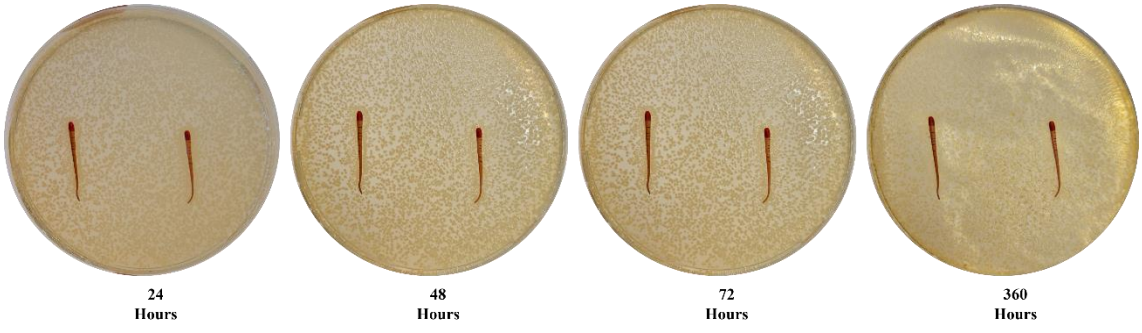

Figure 4.37 Agar plates of CHX-TCS-$FeCl_3$ *E.coli* samples

Opposed to *E.coli*, *S.epidermidis* was successfully eliminated from all coated gutta perchas. One of the main reasons for such success can be related Gram-positive structure

of the bacteria. Since such bacteria don't have an extra protective and resistant layer on the outer surface and are therefore more susceptible to direct interaction between antibacterial agents they're more exposed to the direct effect of the chemicals. The other significant reason is related to the antimicrobial efficacy of both triclosan and chlorhexidine. Since, as it was seen from the inoculation results from the previous section *S.epidermidis* was always successfully inhibited with all coatings.

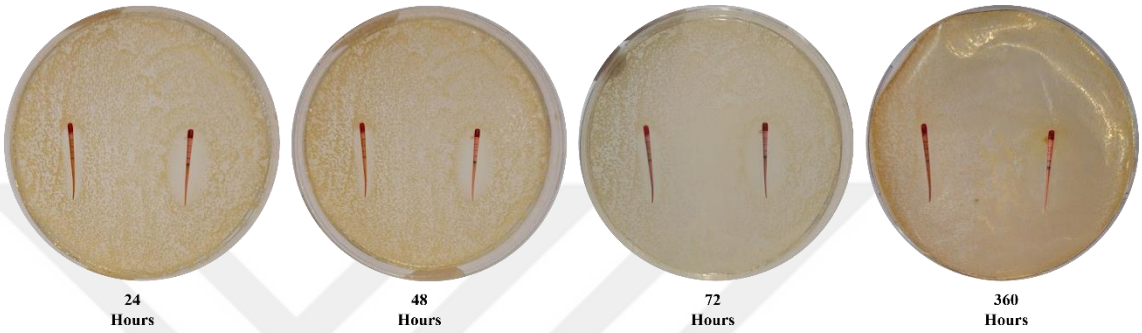

Figure 4.38 Agar plates of CHX-FeCl3 Methanol Washed *S.epidermidis* samples

Compared to methanol rinsed samples, the following samples demonstrated quite adequate inhibition zones. From the results, it's quite clear that both of the monomers were more effective against *S.epidermidis* than *E.coli*.

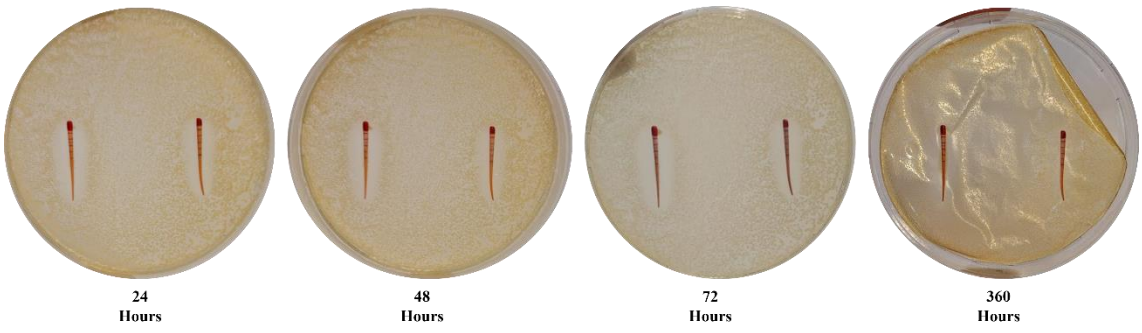

Figure 4.39 Agar plates of CHX-$FeCl_3$ *S.epidermidis* samples

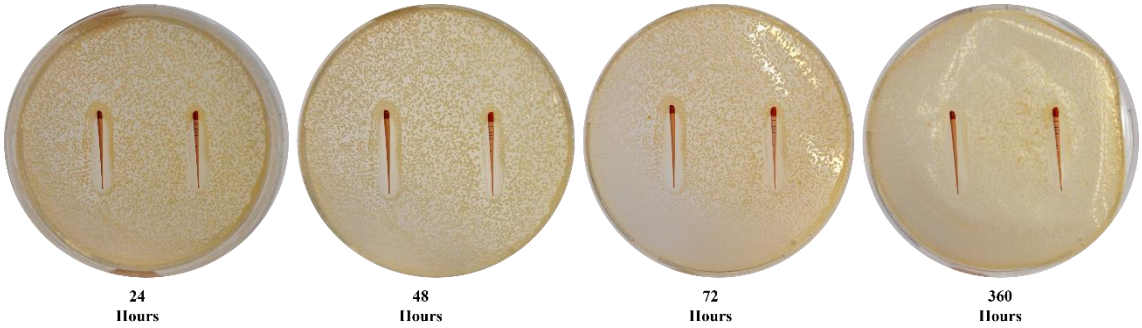

Figure 4.40 Agar plates of CHX-TCS-$FeCl_3$ Methanol Washed *S. mirabilis* samples

Figure 4.41 Agar plates of CHX-TCS-$FeCl_3$ *S. mirabilis* samples

4.4 *In vitro* Cytotoxicity Analysis

As mentioned in the methods section, cytotoxicity tests have been performed according to ISO 10993-5 standard. Resultant cell viability results have been demonstrated in Figure 4.38. In the literature the threshold level for cell viability specified a 70%, if the viability level is lower than this value tested materials accepted as cytotoxic on the contrary if the resultant viability level is higher than 70% then material can be used safely (Cannella et al., 2019).

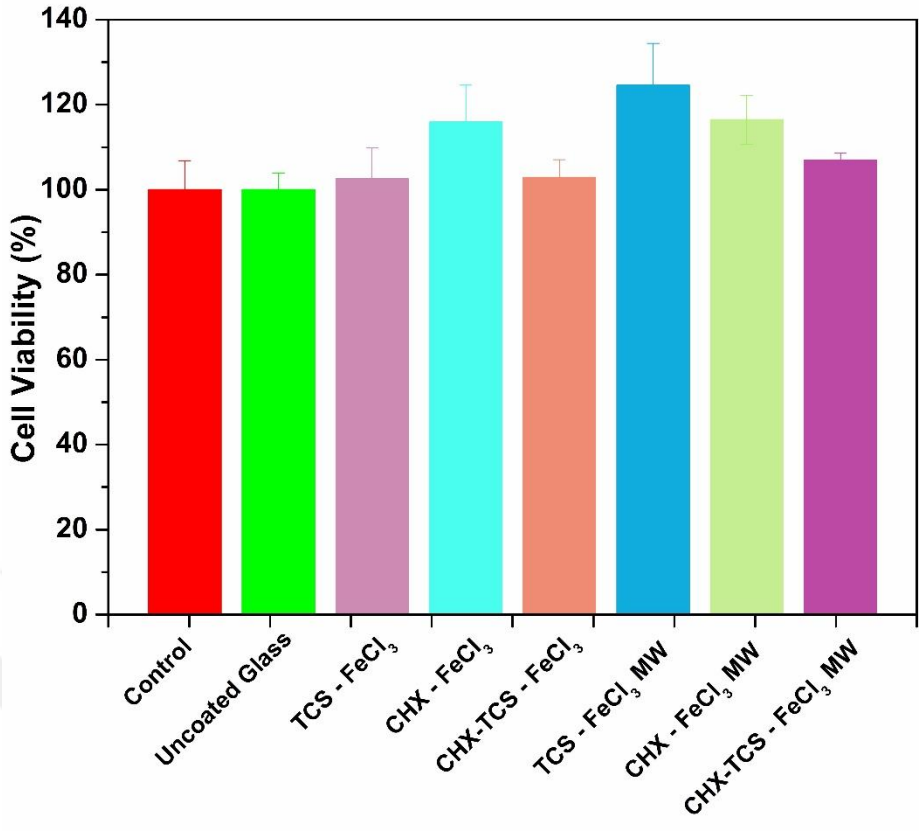

Figure 4.42 Cell Viability difference between thin film coatings. The control sample stands for the (tissue culture polystyrene) which is a standard control sample used in literature

As Figure 4.38 analysed, standard control (tissue culture polystyrene) and the uncoated glass slide samples have had cell viability with 100% viability. When the viability of the thin films analysed all of the thin films had significant viability results with the lowest rate being 102.51% on the TCS – $FeCl_3$ coated films and the highest being the TCS – $FeCl_3$ methanol rinsed samples with 124.57% viability. The remaining viability levels vary between these two percentages.

When viability levels reach such high values, it indicates certain advantages of the materials to be tested. Firstly, it indicates that tested materials are highly biocompatible and do not elicit any immune mechanism when utilized on real tissues. Besides, material helps to improve the survival capabilities of the cells therefore it'll eventually lead to growth and proliferation of the host cells. This is quite significant in medical devices

when contacting with actual tissues. Additionally, being highly biocompatible also helps to proper integration of medical devices or materials with the tissues to be contacted therefore all the possible immune responses like inflammation, pain, and sores can be eliminated. Correspondingly, all TCS and CHX thin films can be used safely for medical purposes.

5. CONCLUSION

In the study, the antimicrobial efficiency of TCS and CHX chemicals was combined and coated on gutta percha surfaces with oCVD method. Gutta perchas are thermoplastic materials that have been used for filling the remaining vacancy after root cleaning in root canal treatment. Since the tooth has vital tissues such as blood vessels and nerves, it can produce moisture and there is a constant flow of nutrients. Due to their affluent condition tooth roots are constantly susceptible to bacterial invasion. if essential care is not taken bacteria can easily spread and cause infection and by time it causes tooth decay. In such cases, RCT comes into play where all the infected tissues have been removed and the remaining openings were filled with gutta percha and adhesive agents.

In some cases, even though infected tissues have been removed, residual bacteria which was not able to be removed can repopulate and cause secondary infection which leads to secondary RCT. In such cases, treatment has to be repeated and due to the spreading of bacteria over time, healthy teeth are also in danger of being infected. In order to prevent such damaging processes in this study antimicrobial efficiency proven chemicals have been used. The main target of the study was inhibiting bacterial existence on vital teeth tissue and preventing their further damage to healthy tissues. Therefore, to improve the success of RCT gutta percha surfaces were coated with a copolymer thin film that can eliminate bacterial formations on roots. The target bacteria were *E.coli* and *S.epidermidis* which are both present in roots and cause the formation of infection leading to secondary root canal treatment.

Following the successful thin film coatings on gutta percha surfaces, morphological and structural analysis have been done with FTIR, UV-Vis, XPS, ToF-SIMS and SEM. In structural analysis, thin films had strong similarity to the monomer chemicals and it was concluded that during copolymerization chains were bonded with each other with -C-Cl, C-N, and C=N bonds with few being from aromatic rings. The surface of the coatings exhibited homogenous coatings which were one of the key points for utilizing oCVD. In addition to structural analysis, coated gutta perchas were tested for their intended inhibitor

and protective actions. Antimicrobial studies were carried out for 15 days. For both bacteria, inhibition rates were sufficient with the rates varying between 61.3% to 99.9% for both bacteria that were adhered to surfaces and the ones that survived on the feedlot. Additionally, zone of inhibition tests demonstrated the repellent action of coatings. Aside from prosperous inhibitive results, thin film coatings were also tested for their biocompatibility (cytotoxicity) with mouse fibroblast cells. In all five repetitions, all coatings had quite high cell viability results with 102% being the minimum and reaching up to 124% which indicates the coatings don't have any damaging effect on cells. Additionally, they didn't induce the defence mechanism of cells.

In the view of results, the intended results have been accomplished. For future studies, the applicability of the coatings is planned to be tested on different bacteria and fungi. With positive results, utilization areas are going to be expanded to different medical equipments. To achieve such a target further investigation of the biocompatibility should be investigated with protein adsorption studies.

REFERENCES

Aminu, N., Chan, S. Y., Mumuni, M. A., Umar, N. M., Tanko, N., Zauro, S. A., Aminu, A., & Toh, S. M. (2021). Physicochemical compatibility studies of triclosan and flurbiprofen with excipients of pharmaceutical formulation using binary, ternary, and multi-combination approach. *Future Journal of Pharmaceutical Sciences*, *7*(1).

Arola, D. D., Gao, S., Zhang, H., & Masri, R. (2017). The Tooth: Its Structure and Properties. *Dent Clin North Am*, *61*(4), 651-668.

Aslam, J., Aslam, J., Verma, C., Hussain, C. M., & Knovel. (2023). *Electrochemical and analytical techniques for sustainable corrosion monitoring : advances, challenges and opportunities*. Elsevier.

Banci, H. A., Strazzi-Sahyon, H. B., Bento, V. A. A., Sayeg, J. M. C., Bachega, M. O., Pellizzer, E. P., & Sivieri-Araujo, G. (2023). Influence of antimicrobial photodynamic therapy on the bond strength of endodontic sealers to intraradicular dentin: A systematic review and meta-analysis. *Photodiagnosis Photodyn Ther*, *41*, 103270.

Beamson, G. (1992). High Relution XPS of Organic Polymers. The Scienta ESCA 300 Database. *ICIplc*.

Belu, A. M., Graham, D. J., & Castner, D. G. (2003). Time-of-flight secondary ion mass spectrometry: techniques and applications for the characterization of biomaterial surfaces. *Biomaterials*, *24*(21), 3635-3653.

Bergenholtz, G. (2016). Assessment of treatment failure in endodontic therapy. *J Oral Rehabil*, *43*(10), 753-758.

Bettencourt, A. F., Costa, J., Ribeiro, I. A. C., Gonçalves, L., Arias-Moliz, M. T., Dias, J. R., Franco, M., Alves, N. M., Portugal, J., & Neves, C. B. (2023). Development of a chlorhexidine delivery system based on dental reline acrylic resins. *International Journal of Pharmaceutics*, *631*.

Bhargava, H. N., & Leonard, P. A. (1996). Triclosan: applications and safety. *Am J Infect Control*, *24*(3), 209-218.

Borrelli, D. C., Barr, M. C., Bulovic, V., & Gleason, K. K. (2012). Bilayer heterojunction polymer solar cells using unsubstituted polythiophene via oxidative chemical vapor deposition. *Solar Energy Materials and Solar Cells*, *99*, 190-196.

Brescó, M. S., Harris, L. G., Thompson, K., Stanic, B., Morgenstern, M., O'Mahony, L., Richards, R. G., & Moriarty, T. F. (2017). Pathogenic Mechanisms and Host Interactions in

Brookes, Z. L. S., Bescos, R., Belfield, L. A., Ali, K., & Roberts, A. (2020). Current uses of chlorhexidine for management of oral disease: a narrative review. *J Dent*, *103*, 103497.

Cannella, V., Altomare, R., Chiaramonte, G., Di Bella, S., Mira, F., Russotto, L., Pisano, P., & Guercio, A. (2019). Cytotoxicity Evaluation of Endodontic Pins on L929 Cell Line. *Biomed Res Int*, *2019*, 3469525.

Celebioglu, A., Umu, O. C. O., Tekinay, T., & Uyar, T. (2014). Antibacterial electrospun nanofibers from triclosan/cyclodextrin inclusion complexes. *Colloids and Surfaces B-Biointerfaces*, *116*, 612-619.

Chandler, N. (2010). Root canal filling. *Harty's endodontics in clinical practice. 6th ed. Edinburgh: Elsevier*, 131-157.

Creighton, J., & Ho, P. (2001). Introduction to chemical vapor deposition (CVD). *ASM International*, *407*.

Deo, P. N., & Deshmukh, R. (2019). Oral microbiome: Unveiling the fundamentals. *J Oral Maxillofac Pathol*, *23*(1), 122-128.

Devang Divakar, D., Muzaheed, Aldeyab, S. S., Alfawaz, S. A., AlKheraif, A. A., & Ahmed Khan, A. (2017). High proportions of Staphylococcus epidermidis in dental caries harbor multiple classes of antibiotics resistance, significantly increase inflammatory interleukins in dental pulps. *Microb Pathog*, *109*, 29-34.

Device-Related Infection. *Frontiers in Microbiology*, *8*.

Dianatdar, A., & Bose, R. K. (2023). Oxidative chemical vapor deposition for synthesis and processing of conjugated polymers: a critical review. *Journal of Materials Chemistry C*, *11*(35), 11776-11802.

Doll, G. L., Mensah, B. A., Mohseni, H., & Scharf, T. W. (2010). Chemical Vapor Deposition and Atomic Layer Deposition of Coatings for Mechanical Applications. *Journal of Thermal Spray Technology*, *19*(1-2), 510-516.

Dorfer, C., Benz, C., Aida, J., & Campard, G. (2017). The relationship of oral health with general health and NCDs: a brief review. *Int Dent J*, *67 Suppl 2*(Suppl 2), 14-18.

Dutta, A. (2017). Fourier transform infrared spectroscopy. *Spectroscopic methods for nanomaterials characterization*, 73-93.

Dutta, R., Tian, S. I. P., Liu, Z., Lakshminarayanan, M., Venkataraj, S., Cheng, Y., Bash, D., Chellappan, V., Buonassisi, T., & Jayavelu, S. (2022). Extracting film thickness and optical constants from spectrophotometric data by evolutionary optimization. *PLoS One*, *17*(11), e0276555.

Estrela, C., Holland, R., Estrela, C. R., Alencar, A. H., Sousa-Neto, M. D., & Pecora, J. D. (2014). Characterization of successful root canal treatment. *Braz Dent J*, *25*(1), 3-11.

Faran Ali, S. M., & Tanwir, F. (2012). Oral microbial habitat a dynamic entity. *J Oral Biol Craniofac Res*, *2*(3), 181-187.

Fotovvati, B., Namdari, N., & Dehghanghadikolaei, A. (2019). On Coating Techniques for Surface Protection: A Review. *Journal of Manufacturing and Materials Processing*, *3*(1).

Fraga, M., & Pessoa, R. (2020). Progresses in Synthesis and Application of SiC Films: From CVD to ALD and from MEMS to NEMS. *Micromachines*, *11*(9).

Friedlander, A. H. (2010). Oral cavity staphylococci are a potential source of prosthetic joint infection. *Clin Infect Dis*, *50*(12), 1682-1683; author reply 1683.

Gajan, E. B., Aghazadeh, M., Abashov, R., Salem Milani, A., & Moosavi, Z. (2009). Microbial Flora of Root Canals of Pulpally-infected Teeth: Enterococcus faecalis a Prevalent Species. *J Dent Res Dent Clin Dent Prospects*, *3*(1), 24-27.

Ghahramani, S., Ziar, N., Moradi, N., Bagheri Lankarani, K., & Sayari, M. (2022). Preserving natural teeth versus extracting them: a willingness to pay analysis. *BMC Oral Health*, *22*(1), 375.

Graham, D. J., & Gamble, L. J. (2023). Back to the basics of time-of-flight secondary ion mass spectrometry of bio-related samples. I. Instrumentation and data collection. *Biointerphases*, *18*(2), 021201.

Gross, E. L., Beall, C. J., Kutsch, S. R., Firestone, N. D., Leys, E. J., & Griffen, A. L. (2012). Beyond Streptococcus mutans: dental caries onset linked to multiple species by 16S rRNA community analysis. *PLoS One*, *7*(10), e47722.

Haque, M., Sartelli, M., & Haque, S. Z. (2019). Dental Infection and Resistance-Global Health Consequences. *Dent J (Basel)*, *7*(1).

Hashmi, S. (2014). Comprehensive Materials Processing Preface. *Comprehensive Materials Processing, Vol 1: Assessing Properties of Conventional and Specialized Materials*, Xxvii-Xxvii.

Hofstetter, Y. J., & Vaynzof, Y. (2019). Quantifying the damage induced by x-ray photoelectron spectroscopy depth profiling of organic conjugated polymers. *ACS Applied Polymer Materials*, *1*(6), 1372-1381.

Inkson, B. J. (2016). Scanning electron microscopy (SEM) and transmission electron microscopy (TEM) for materials characterization. In *Materials characterization using nondestructive evaluation (NDE) methods* (pp. 17-43). Elsevier.

Ismail, A. A., van de Voort, F. R., & Sedman, J. (1997). Fourier transform infrared spectroscopy: principles and applications. In *Techniques and instrumentation in analytical chemistry* (Vol. 18, pp. 93-139). Elsevier.

ISO. (2022). *ISO 10993-5:2009, Biological evaluation of medical devices, Part 5: Tests for in vitro cytotoxicity*. International Organization for Standardization.

Jang, Y. E., Kim, Y., Kim, S. Y., & Kim, B. S. (2024). Predicting early endodontic treatment failure following primary root canal treatment. *BMC Oral Health*, *24*(1), 327.

Jenkins, S., Addy, M., & Newcombe, R. (1993). The effects of a chlorhexidine toothpaste on the development of plaque, gingivitis and tooth staining. *J Clin Periodontol*, *20*(1), 59-62.

Jongsma, M. A., van der Mei, H. C., Atema-Smit, J., Busscher, H. J., & Ren, Y. (2015). In vivo biofilm formation on stainless steel bonded retainers during different oral health-care regimens. *Int J Oral Sci*, *7*(1), 42-48.

Kamay, İ. C. (2015). Diş çürüğü ve tarihteki öyküsü. *Antropoloji*(29), 17-28.

Karak, N. (2019). Silver nanomaterials and their polymer nanocomposites. In *Nanomaterials and polymer nanocomposites* (pp. 47-89). Elsevier.

Karpiński, T., & Szkaradkiewicz, A. (2015). Chlorhexidine–pharmaco-biological activity and application. *Eur Rev Med Pharmacol Sci*, *19*(7), 1321-1326.

Kaur, A., Shah, N., Logani, A., & Mishra, N. (2015). Biotoxicity of commonly used root canal sealers: A meta-analysis. *J Conserv Dent*, *18*(2), 83-88.

Kibret, M., & Abera, B. (2011). Antimicrobial susceptibility patterns of *E.coli* from clinical sources in northeast Ethiopia. *Afr Health Sci*, *11 Suppl 1*(Suppl 1), S40-45.

Kumar, D. S., Kumar, B. J., & Mahesh, H. (2018). Quantum nanostructures (QDs): an overview. *Synthesis of inorganic nanomaterials*, 59-88.

Li, M., He, Y., Sun, J., Li, J., Bai, J., & Zhang, C. (2019). Chronic Exposure to an Environmentally Relevant Triclosan Concentration Induces Persistent Triclosan Resistance but Reversible Antibiotic Tolerance in Escherichia coli. *Environ Sci Technol*, *53*(6), 3277-3286.

Li, P., Xuan, Y., Jiang, B., Zhang, S., & Xia, C. (2022). Hollow La0. 6Sr0. 4Ni0. 2Fe0. 75Mo0. 05O3-δ electrodes with exsolved FeNi3 in quasi-symmetrical solid oxide electrolysis cells for direct CO2 electrolysis. *Electrochemistry Communications*, *134*, 107188.

Lou, Y. J., Cai, H., Liu, X., Tu, S. C., Pei, K., Zhao, Y. Y., Cao, G., Li, S. L., Qin, K. M., & Cai, B. C. (2014). Element analysis and characteristic identification of non-fumigated and sulfur-fumigated using microwave digestion-inductively coupled plasma atomic emission spectrometry combined with Fourier transform infrared spectrometry. *Pharmacognosy Magazine*, *10*(37), S30-S36.

Lu, J., Jin, M., Nguyen, S. H., Mao, L., Li, J., Coin, L. J. M., Yuan, Z., & Guo, J. (2018). Non-antibiotic antimicrobial triclosan induces multiple antibiotic resistance through genetic mutation. *Environ Int*, *118*, 257-265.

Macri, D. (2017). Worldwide Use of Triclosan: Can Dentistry Do Without this Antimicrobial? *Contemp Clin Dent*, *8*(1), 7-8.

Marsh, P. D. (2010). Microbiology of dental plaque biofilms and their role in oral health and caries. *Dent Clin North Am*, *54*(3), 441-454.

Méndez-Vilas, A. (2011). *Science against microbial pathogens: communicating current research and technological advances* (Vol. 1). Formatex Research Center Badajoz.

Milani, E. S., Hasani, A., Varschochi, M., Sadeghi, J., Memar, M. Y., & Hasani, A. (2021). Biocide resistance in Acinetobacter baumannii: appraising the mechanisms. *J Hosp Infect*, *117*, 135-146.

Minuti, A. E., Labusca, L., Herea, D. D., Stoian, G., Chiriac, H., & Lupu, N. (2022). A Simple Protocol for Sample Preparation for Scanning Electron Microscopic Imaging Allows Quick Screening of Nanomaterials Adhering to Cell Surface. *Int J Mol Sci*, *24*(1).

Mohammed, A., & Abdullah, A. (2018). Scanning electron microscopy (SEM): A review. Proceedings of the 2018 International Conference on Hydraulics and Pneumatics—HERVEX, Băile Govora, Romania,

Morris, A. L., & Tadi, P. (2024). Anatomy, Head and Neck, Teeth. In *StatPearls*.

Noc, L., & Jerman, I. (2022). Review of the spectrally selective (CSP) absorber coatings, suitable for use in SHIP. *Solar Energy Materials and Solar Cells*, *238*.

Onnainty, R., Onida, B., Páez, P., Longhi, M., Barresi, A., & Granero, G. (2016). Targeted chitosan-based bionanocomposites for controlled oral mucosal delivery of chlorhexidine. *International Journal of Pharmaceutics*, *509*(1-2), 408-418.

Ooi, H. Y., Tee, W. Y., Davamani, F., & Nagendrababu, V. (2019). Comparing the antimicrobial efficacy of pediocin with chlorhexidine and calcium hydroxide as intracanal medicaments against persistent root canal infections. *J Conserv Dent*, *22*(3), 241-244.

Otsuki, A., & ScienceDirect. (2024). *Non-destructive material characterization methods* (1st ed.). Elsevier.

Pavia, D. L., Lampman, G. M., Kriz, G. S., & Vyvyan, J. R. (2015). *Introduction to spectroscopy* (Fifth edition. ed.). Cengage Learning.

Petersen, P. E., World Health, O., & Programme, W. H. O. G. O. H. (2003). *The World oral health report 2003 : continuous improvement of oral health in the 21st century : the approach of the WHO Global Oral Health Programme*. World Health Organization.

Pinto, G., Silva, F., Porteiro, J., Míguez, J., & Baptista, A. (2018). Numerical Simulation Applied to PVD Reactors: An Overview. *Coatings*, *8*(11).

Poppolo Deus, F., & Ouanounou, A. (2022). Chlorhexidine in Dentistry: Pharmacology, Uses, and Adverse Effects. *Int Dent J*, *72*(3), 269-277.

Priyadarshini, B. M., Selvan, S. T., Narayanan, K., & Fawzy, A. S. (2017). Characterization of Chlorhexidine-Loaded Calcium-Hydroxide Microparticles as a Potential Dental Pulp-Capping Material. *Bioengineering (Basel)*, *4*(3).

Qin, X., Zi, H., & Zeng, X. (2022). Changes in the global burden of untreated dental caries from 1990 to 2019: A systematic analysis for the Global Burden of Disease study. *Heliyon*, *8*(9), e10714.

Querido, M. M., Paulo, I., Hariharakrishnan, S., Rocha, D., Pereira, C. C., Barbosa, N., Bordado, J. M., Teixeira, J. P., & dos Santos, R. G. (2021). Auto-Disinfectant Acrylic Paints Functionalised with Triclosan and Isoborneol-Antibacterial Assessment. *Polymers*, *13*(13).

Refai, M., Abdel Hamid, Z., El-Kilani, R. M., & Nasr, G. E. (2020). Reducing the wear and corrosion of the agricultural mower steel knives by electrodeposition nanocomposite coatings–Review. *Egyptian journal of chemistry*, *63*(8), 3075-3095.

Rodrigo, L. (2020). *E.coli infections : importance of early diagnosis and efficient treatment*. IntechOpen.

Roode, G. J., & Butow, K. W. (2018). A Descriptive Study of Chlorhexidine as a Disinfectant in Cleft Palate Surgery. *Clin Med Res*, *16*(1-2), 9-15.

Sasser, L. (2020). Endodontic Disinfection for Orthograde Root Canal Treatment in Veterinary Dentistry. *J Vet Dent*, *37*(1), 35-40.

Selwitz, R. H., Ismail, A. I., & Pitts, N. B. (2007). Dental caries. *The Lancet*, *369*(9555), 51-59.

Shukla, B., Howell, V., Griffiths, A., Thoppil, A., Liu, M., Carter, J., & Young, P. (2014). Superiority of chlorhexidine 2%/alcohol 70% wipes in decontaminating ultrasound equipment. *Ultrasound*, *22*(3), 135-140.

Siqueira, J. F., Jr. (2001). Aetiology of root canal treatment failure: why well-treated teeth can fail. *Int Endod J*, *34*(1), 1-10.

Siqueira, J. F., Jr., Rocas, I. N., Souto, R., Uzeda, M., & Colombo, A. P. (2001). Microbiological evaluation of acute periradicular abscesses by DNA-DNA hybridization. *Oral Surg Oral Med Oral Pathol Oral Radiol Endod*, *92*(4), 451-457.

Siqueira Jr, J., & Rôças, I. (2009). Diversity of endodontic microbiota revisited. *Journal of dental research*, *88*(11), 969-981.

Smith, B. C. (2011). *Fundamentals of Fourier transform infrared spectroscopy* (2nd ed.). CRC Press.

Sodhi, R. N. (2004). Time-of-flight secondary ion mass spectrometry (TOF-SIMS):--versatility in chemical and imaging surface analysis. *Analyst*, *129*(6), 483-487.

Sodhi, R. N., Grad, H. A., & Smith, D. C. (1992). Examination by X-ray photoelectron spectroscopy of the adsorption of chlorhexidine on hydroxyapatite. *J Dent Res*, *71*(8), 1493-1497.

Stevie, F. A., & Donley, C. L. (2020). Introduction to x-ray photoelectron spectroscopy. *Journal of Vacuum Science & Technology A*, *38*(6).

Stuart, B., & ProQuest. (2004). *Infrared spectroscopy : fundamentals and applications* (1st ed.). J. Wiley.

Van der Heide, P. (2012). *X-ray photoelectron spectroscopy : an introduction to principles and practices*. Wiley-Blackwell.

Vickerman, J. C., & Briggs, D. (2013). *ToF-SIMS : materials analysis by mass spectrometry* (2nd edition. ed.). IM Publications.

Vishwanath, V., & Rao, H. M. (2019). Gutta-percha in endodontics-A comprehensive review of material science. *Journal of Conservative Dentistry and Endodontics*, *22*(3), 216-222.

Watts, J. F. (1994). X-ray photoelectron spectroscopy. *Surface science techniques*, *45*(5).

Worsfold, P., Townshend, A., Poole, C. F., & Miró, M. (2019). *Encyclopedia of analytical science* (Third edition ed.). Elsevier.

Wu, H., Gao, G., Zhou, X., Zhang, Y., & Guo, S. (2012). Control on the formation of Fe 3 O 4 nanoparticles on chemically reduced graphene oxide surfaces. *CrystEngComm*, *14*(2), 499-504.

Yadav, K., & Prakash, S. (2017). Dental caries: A microbiological approach. *J Clin Infect Dis Pract*, *2*(1), 1-15.

Yang, L., May, P. W., Yin, L., Smith, J. A., & Rosser, K. N. (2007). Ultra fine carbon nitride nanocrystals synthesized by laser ablation in liquid solution. *Journal of Nanoparticle Research*, *9*(6), 1181-1185.

Zeng, W., Xu, W., Xu, Y., Liao, W., Zhao, Y., Zheng, X., Xu, C., Zhou, T., & Cao, J. (2020). The prevalence and mechanism of triclosan resistance in Escherichia coli isolated from urine samples in Wenzhou, China. *Antimicrob Resist Infect Control*, *9*(1), 161.

Zhang, X. N., Liu, X. Y., Huang, Y. F., Sun, B., Liu, Z. Y., Liao, G. L., & Shi, T. L. (2023). Review on flexible perovskite photodetector: processing and applications. *Frontiers of Mechanical Engineering*, *18*(2).